

## Quiver symmetries and wall-crossing invariance

---

Fabrizio Del Monte<sup>a,b</sup> Pietro Longhi<sup>c</sup>

<sup>a</sup>*Centre de Recherches Mathématiques, Université de Montréal, C. P. 6128, Succ. Centre Ville, Montréal, QC H3C 3J7 Canada*

<sup>b</sup>*Department of Mathematics and Statistics, Concordia University, 1455 de Maisonneuve Blvd. W. Montréal, QC H3G 1M8 Canada*

<sup>c</sup>*Institute for Theoretical Physics, ETH Zurich, 8093, Zurich, Switzerland*

*E-mail:* [delmonte@crm.umontreal.ca](mailto:delmonte@crm.umontreal.ca), [longhip@phys.ethz.ch](mailto:longhip@phys.ethz.ch),

**ABSTRACT:** We study the BPS particle spectrum of five-dimensional superconformal field theories (SCFTs) on  $\mathbb{R}^4 \times S^1$  with one-dimensional Coulomb branch, by means of their associated BPS quivers. By viewing these theories as arising from the geometric engineering within M-theory, the quivers are naturally associated to the corresponding local Calabi-Yau threefold. We show that the symmetries of the quiver, descending from the symmetries of the Calabi-Yau geometry, together with the affine root lattice structure of the flavor charges, provide equations for the Kontsevich-Soibelman wall-crossing invariant. We solve these equations iteratively: the pattern arising from the solution is naturally extended to an exact conjectural expression, that we provide for the local Hirzebruch  $\mathbb{F}_0$ , and local del Pezzo  $dP_3$  and  $dP_5$  geometries. Remarkably, the BPS spectrum consists of two copies of suitable  $4d \mathcal{N} = 2$  spectra, augmented by Kaluza-Klein towers.

---

## Contents

<b>1</b>	<b>Introduction</b>	<b>1</b>
<b>2</b>	<b>Symmetry constraints on wall-crossing invariants</b>	<b>9</b>
2.1	Quivers, stability conditions and BPS states	9
2.2	Collimation chambers	10
2.3	The wall-crossing invariant $\mathbb{U}$	12
2.4	Quiver permutation symmetry	13
2.5	Constraining $\mathbb{U}$	14
<b>3</b>	<b>Affine root lattices and stability conditions</b>	<b>15</b>
3.1	Charge lattices	15
3.2	Affine symmetry from geometry	17
3.3	Cremona isometries, affine translations, and $\text{Aut}_Q$	18
3.4	Stability condition for local del Pezzos from affine translations	20
<b>4</b>	<b>Examples</b>	<b>22</b>
4.1	$\mathbb{F}_0$	22
4.2	$dP_3$	31
4.3	$dP_5$	39

---

## 1 Introduction

The BPS spectral problem in supersymmetric Quantum Field Theories with eight supercharges is a rich subject, with connections to various branches of theoretical and mathematical physics, such as the WKB approximation and Stokes phenomena for Schrödinger equations (and higher order analogues), Donaldson-Thomas invariants in enumerative geometry, and integrable systems both of continuous and discrete types. The past decade has brought remarkable progress on the case of four-dimensional  $\mathcal{N} = 2$  theories [1–10], driven by seminal advances on wall-crossing phenomena [11, 12]. More recently, various groups have started to tackle the problem of describing the spectrum of BPS states of five-dimensional SCFTs, arising from the compactification of M-theory on local Calabi-Yau threefolds, where the BPS states are to be understood as branes wrapping compact cycles of the Calabi-Yau [13–24]. These are the theories we will discuss in the present paper.

Both in four and five dimensions, a key feature of BPS spectra is the wall-crossing phenomenon. As we move along the moduli space of vacua of a theory, the BPS spectrum is only piecewise constant, with discontinuities on codimension-one walls. These walls are loci where stable particles can decay, and they subdivide the moduli space into chambers with different BPS spectra in each of them. Even though the BPS spectrum itself is

not preserved on the whole moduli space, there are still wall-crossing invariant quantities, that are constant and chamber-independent. An important example is the Konsevich-Soibelman (KS) invariant  $\mathbb{U}$ , also known as quantum monodromy or motivic spectrum generator [11]. On the one hand, it is always possible to derive the BPS spectrum in any chamber from  $\mathbb{U}$ . On the other hand,  $\mathbb{U}$  can be computed from knowledge of the BPS spectrum at some point in moduli space. Thanks to its invariance property, it is sufficient to compute  $\mathbb{U}$  in a specific chamber where the spectrum admits a simple description, in order to obtain the spectrum in any other chamber. Our goal will be to compute the spectrum generator for certain five-dimensional SCFTs, by using symmetries of the underlying Calabi-Yau geometry.<sup>1</sup>

Our main tool will be the so-called BPS quiver of the theory [4, 5, 28–32]. This can be thought of as the quiver characterizing the Supersymmetric Quantum Mechanics describing the low-energy dynamics of the BPS states of the theory. The spectrum is then encoded by the associated representation theory for suitable stability conditions. As it turns out, this approach is generically difficult for quivers of the five-dimensional theories considered in this paper, see e.g. [17] for a recent discussion.

An alternative way to obtain the BPS spectrum from a quiver, which has been used to great effect in the four-dimensional case, is the so-called “mutation method” [4, 5]. The idea behind it is that every node in the BPS quiver represents a hypermultiplet BPS state, characterized by a ray in the complex plane of central charges. Since the central charge of an antiparticle is the opposite of the central charge of the corresponding particle, the whole spectrum is encoded by the rays within a half-plane. A choice of half-plane corresponds to a choice of quiver description of the BPS spectrum, for a given point in the moduli space of stability conditions. If one starts to tilt the choice of half-plane, at some point the ray of a BPS state will exit the half-plane, and this will induce a change in the quiver description corresponding to a mutation of the BPS quiver at the corresponding node [33]. We have however done nothing physically meaningful, so the new quiver just corresponds to a dual description of the same physics, so that the charges of the new nodes of the quiver must have been also in the original spectrum. By iterating this procedure, one produces stable hypermultiplet states in a given chamber: multiplets with higher spin content appear as limiting vectors of infinite sequences of mutations, and different chambers in moduli space will correspond to different relative orderings of the phases of central charges. In chambers where all stable BPS states correspond to hypermultiplets, the mutation method exhausts the whole BPS spectrum. This is sometimes the case for BPS quivers of four-dimensional  $\mathcal{N} = 2$  theories, however it is never the case for five-dimensional SCFTs.

While the mutation method is not as powerful in five dimensions as it is in four dimensions, it is nevertheless quite useful in favourable circumstances. On the one hand, it

---

<sup>1</sup>For BPS spectra of 4d  $\mathcal{N} = 2$  theories of class  $\mathcal{S}$ , this task has been accomplished in [2] for theories of type  $A_1$  and a general approach for all class  $\mathcal{S}$  theories was developed in [25]. The latter approach should generalize to 5d  $\mathcal{N} = 1$  theories via exponential networks, as observed in [15, 16]. However, this requires finding a special point in moduli space (the Roman locus of [26]). Existence of such a locus has been discussed recently in the literature [27], it would be interesting to pursue this approach for more general models than those considered here.

was observed in [17] that certain SCFTs admit choices of stability conditions for which the mutation method *almost* captures the full BPS spectrum, leaving out only BPS states with central charges aligned along a single ray in the complex plane. Moreover, it was proposed in [34] that the mutation method should be generalized by exploiting symmetries of the quivers, that can be used to define discrete integrable systems giving rise to q-Painlevé equations [35–38], whose connection with five-dimensional theories was first recognized in a different but related context in [39, 40]. In [41, Appendix] the symmetries of the quiver were used to complete the description of BPS states derived via mutations in [17], for the case of local  $\mathbb{F}_0$ . In this paper we elaborate on these ideas in a more precise and systematic way, and apply them to compute the motivic spectrum generator for certain local Calabi-Yau threefolds whose BPS charges have an underlying structure of an affine root lattice, as it happens for all local del Pezzos<sup>2</sup>. We will focus on the specific examples local  $\mathbb{F}_0$ , and the local del Pezzos  $dP_3, dP_5$ , the latter example being non-toric.

Our main result will be to show that symmetries of a local CY geometry (not necessarily toric) together with wall-crossing invariance, are sometimes enough to constrain the BPS spectrum entirely, leading to exact expressions for  $\mathbb{U}$  and the spectrum, as well as highly nontrivial wall-crossing identities. Two important caveats apply. First, wall-crossing invariance only constrains BPS states whose charges are not pure-flavor, i.e. whose Dirac-Schwinger-Zwanziger (DSZ) pairing with other charges is not identically zero. Our method does not determine BPS states with pure-flavor charges (such as boundstates of D0 branes), these must be obtained by other methods. Our results should be regarded as partially conjectural, admitting the possibility of additional BPS states with pure-flavor charges that we have not detected.<sup>3</sup> Second, we use symmetries of the quiver and wall-crossing invariance to derive exact equations for  $\mathbb{U}$ , which we solve iteratively, leading to partial descriptions of the BPS spectrum. We then complete these descriptions by observing certain patterns in the spectrum, namely certain periodicities, leading to a *conjectural* expression for  $\mathbb{U}$ .

With these caveats in mind, we arrive at explicit and exact (conjectural) descriptions of the BPS spectrum. The starting point for our approach is the observation that the so-called Cremona group  $\text{Cr}(dP_n)$  of del Pezzo surfaces  $dP_n$  [42], are realized by the extended affine Weyl group  $\widetilde{W}(E_n^{(1)})$  (there can be an extra finite group factor, see Section 3.4 for details) acting on the BPS charge lattice of the theory through sequences of mutations and permutations that leave the quiver invariant. These transformations form the automorphism group of the quiver  $\text{Aut}_Q$ , so that

$$\text{Aut}_Q \approx \text{Cr}(dP_n) \supseteq \widetilde{W}(E_n^{(1)}) = \left( W(E_n) \rtimes \mathcal{T}(E_n^{(1)}) \right) \times \text{Out}(E_n^{(1)}), \quad (1.1)$$

---

<sup>2</sup>Local del Pezzos are open Calabi-Yau threefolds arising as total space of the canonical bundle over a del Pezzo surface. The del Pezzo surface  $dP_n$  is a two-dimensional complex surface obtained by blowing up  $\mathbb{P}^2$  at  $n$  generic points.

<sup>3</sup>For the case of local  $\mathbb{F}_0$  we believe the result to be exhaustive, based on comparisons with exponential networks in [41]. More generally, the ambiguity on pure-flavor states may be related to the fact that our approach is independent of a choice of superpotential associated to a quiver. It is expected that different choices of superpotentials would result in different BPS spectra. The difference should then lie in the spectrum of pure-flavor states, while the part of the spectrum that we compute should be independent of such a choice.

where we decomposed the extended affine Weyl group into affine translations  $\mathcal{T}$ , simple reflections  $W$ , and Dynkin diagram automorphisms  $\text{Out}(E_n^{(1)})$ . Among these transformations, a special role is taken by affine translations  $\mathcal{T}(E_n^{(1)})$ , that can be thought of as discrete time evolutions on the BPS charges, and by the subgroup  $\Pi_Q$  of quiver automorphisms consisting only of permutations on the nodes.<sup>4</sup>

We will show that it is possible to identify certain affine translations with tiltings of the upper half-plane corresponding to an appropriate stability condition, so that we associate to an affine translation a chamber in the moduli space of the theory. Furthermore, we will show that the chambers obtained this way have the ‘‘collimation’’ property: this means that their spectrum is organized into towers of hypermultiplets, with all the higher-spin BPS states aligned on the real axis of the complex plane of BPS central charges. The motivic spectrum generator in such a chamber is factorized as

$$\mathbb{U} = \mathbb{U}(\angle^+) \cdot \mathbb{U}(\mathbb{R}^+) \cdot \mathbb{U}(\angle^-), \quad (1.2)$$

where  $\mathbb{U}(\angle^\pm)$  are the contributions from BPS states with central charges lying inside the first quadrant and fourth quadrant respectively, while  $\mathbb{U}(\mathbb{R}^+)$  contains the contribution of the rays lying on the positive real axis. We will show that the affine translations fully determine  $\mathbb{U}(\angle^\pm)$ , while  $\mathbb{U}(\mathbb{R}^+)$  can be fixed using the remaining transformations of  $\text{Aut}_Q \approx \text{Cr}(dP_n)$ . This is done by noting that the permutation symmetry group  $\Pi_Q \subset \text{Aut}_Q$  of the quiver contains transformations that are automorphisms of the Dynkin diagram. Denoting such a transformation by  $\pi$ , this has the effect of relating different affine translations  $T, T'$  as

$$T' = \pi^{-1} T \pi. \quad (1.3)$$

As a result, the collimation chambers  $\mathcal{C}, \mathcal{C}'$  constructed from the two translations  $T$  and  $T'$  will be simply related by the permutation  $\pi$  of the charge vectors. This statement, combined with wall-crossing invariance and the factorization (1.2), allows us to compute  $\mathbb{U}(\mathbb{R}^+)$  recursively from

$$\mathbb{U}[\mathcal{C}] = \mathbb{U}[\mathcal{C}'] = \mathbb{U}[\pi(\mathcal{C})]. \quad (1.4)$$

For the cases we consider, the affine translations naturally split the BPS in quiver into two four-dimensional quivers: this was first noticed in [34], and is shown in Figure 1. As we will discuss shortly, this is reflected in the full BPS spectrum.

## Main results

Solving equation (1.4) for suitable chambers of local  $\mathbb{F}_0, dP_3, dP_5$  we obtain the following conjectural BPS spectra.<sup>5</sup>

For local  $\mathbb{F}_0$  we choose generators  $\gamma_i$  of the charge lattice corresponding to nodes of the BPS quivers shown in Figure 1a. In a chamber where

$$Z_{\gamma_1} = Z_{\gamma_3}, \quad Z_{\gamma_2} = Z_{\gamma_4}, \quad \arg Z_{\gamma_1} > \arg Z_{\gamma_2}, \quad Z_{\gamma_1} + Z_{\gamma_2} \in \mathbb{R}^+, \quad (1.5)$$

<sup>4</sup>In the context of 4d  $\mathcal{N} = 2$  theories, the time evolution of discrete integrable systems associated to BPS quivers was related to the study of BPS spectra in [43–45]

<sup>5</sup>As mentioned earlier, BPS states with pure-flavor charges go undetected by the wall-crossing identity (1.4). These states, which include boundstates of D0 branes, can’t be determined by wall-crossing invariance, since such states do not participate in wall-crossing.

we find the following BPS spectrum

$\gamma$	$\Omega(\gamma; y)$
$\gamma_1 + k(\gamma_1 + \gamma_2)$	1
$-\gamma_1 + (k+1)(\gamma_1 + \gamma_2)$	1
$\gamma_3 + k(\gamma_3 + \gamma_4)$	1
$-\gamma_3 + (k+1)(\gamma_3 + \gamma_4)$	1
$\gamma_1 + \gamma_2 + k\gamma_{D0}$	$y + y^{-1}$
$-\gamma_1 - \gamma_2 + (k+1)\gamma_{D0}$	$y + y^{-1}$
$(k+1)\gamma_{D0}$	$y^3 + 2y + y^{-1}$

(1.6)

where  $\gamma_{D0} = \sum_{i=1}^4 \gamma_i$ . The spectrum also includes the respective antiparticles obtained by sending  $\gamma \rightarrow -\gamma$ . Note that this spectrum consists of two copies of the weakly coupled spectrum of pure  $SU(2)$  SYM in 4d [5], with the extra KK towers in lower part of the table. We also observe that the spectrum is organized into towers over  $\gamma_1, \gamma_3$  and  $\gamma_1 + \gamma_2, \gamma_{D0}$  with steps  $\gamma_1 + \gamma_2, \gamma_3 + \gamma_4$  and  $\gamma_{D0}$ . This structure is strongly reminiscent of the ‘‘peacock patterns’’ observed in [46], where the possibility of a relation to BPS/DT invariants of local CY threefolds is also contemplated. (Also see Figures 4, 7).

For local  $dP_3$  we choose generators  $\gamma_i$  of the charge lattice corresponding to nodes of the BPS quivers shown in Figure 1b. In a chamber where

$$\begin{aligned} Z_{\gamma_1} = Z_{\gamma_4}, \quad Z_{\gamma_2} = Z_{\gamma_5}, \quad Z_{\gamma_3} = Z_{\gamma_6}, \\ \arg Z_{\gamma_1} > \arg Z_{\gamma_2} > \arg Z_{\gamma_3}, \quad Z_{\gamma_1} + Z_{\gamma_3} = Z_{\gamma_2} \in \mathbb{R}^+. \end{aligned} \quad (1.7)$$

we find the following BPS spectrum

$\gamma$	$\Omega(\gamma; y)$
$\gamma_r + k(\gamma_1 + \gamma_2 + \gamma_3)$	1
$-\gamma_r + (k+1)(\gamma_1 + \gamma_2 + \gamma_3)$	1
$\gamma_s + k(\gamma_4 + \gamma_5 + \gamma_6)$	1
$-\gamma_s + (k+1)(\gamma_4 + \gamma_5 + \gamma_6)$	1
$\gamma_t + k\gamma_{D0}$	1
$-\gamma_t + (k+1)\gamma_{D0}$	1
$\gamma_a + \gamma_b + k\gamma_{D0}$	1
$-\gamma_a - \gamma_b + (k+1)\gamma_{D0}$	1
$\gamma_1 + \gamma_2 + \gamma_3 + k\gamma_{D0}$	$y + y^{-1}$
$-\gamma_1 - \gamma_2 - \gamma_3 + (k+1)\gamma_{D0}$	$y + y^{-1}$
$(k+1)\gamma_{D0}$	$y^3 + 4y + y^{-1}$

(1.8)

with  $k \geq 0$  and

$$r \in \{1, 3\} \quad s \in \{4, 6\} \quad t \in \{2, 5\} \quad (a, b) \in \{(1, 3), (4, 6)\}. \quad (1.9)$$

where  $\gamma_{D0} = \sum_{i=1}^6 \gamma_i$ , and again the spectrum also includes the respective antiparticles obtained by sending  $\gamma \rightarrow -\gamma$ . This spectrum consists of two copies of the weakly coupled

spectrum of  $SU(2)$  SQCD with one fundamental hypermultiplet in 4d [5], with the extra KK towers in lower part of the table. This is quite striking, since the low-energy gauge theory phase of this SCFT is five-dimensional  $N_f = 2$   $SU(2)$  gauge theory. As for local  $\mathbb{F}_0$ , we observe that the spectrum is organized into towers, over  $\gamma_r, \gamma_s$  and  $\gamma_t, \gamma_a + \gamma_b, \gamma_1 + \gamma_2 + \gamma_3, \gamma_{D0}$  with steps  $\gamma_1 + \gamma_2 + \gamma_3, \gamma_4 + \gamma_5 + \gamma_6$  and  $\gamma_{D0}$ . This structure is reminiscent of the “peacock patterns” observed in [46].

For local  $dP_5$  we choose generators  $\gamma_i$  of the charge lattice corresponding to nodes of the BPS quivers shown in Figure 1c. In a chamber where

$$\begin{aligned} Z_{\gamma_2} = Z_{\gamma_6} = c \cdot Z_{\gamma_1} = c \cdot Z_{\gamma_5}, \quad Z_{\gamma_4} = Z_{\gamma_8} = c \cdot Z_{\gamma_3} = c \cdot Z_{\gamma_7}, \\ Z_{\gamma_1} = \bar{Z}_{\gamma_3}, \quad \arg Z_{\gamma_1} > \arg Z_{\gamma_3}, \end{aligned} \quad (1.10)$$

with an arbitrary real constant  $c > 1$ , needed to ensure that  $Z_{\alpha_i}$  belong to the positive half-plane, we find the following BPS spectrum

$\gamma$	$\Omega(\gamma; y)$
$\gamma_r + k(\gamma_1 + \gamma_2 + \gamma_3 + \gamma_4)$	1
$-\gamma_r + (k+1)(\gamma_1 + \gamma_2 + \gamma_3 + \gamma_4)$	1
$\gamma_s + k(\gamma_5 + \gamma_6 + \gamma_7 + \gamma_8)$	1
$-\gamma_s + (k+1)(\gamma_5 + \gamma_6 + \gamma_7 + \gamma_8)$	1
$\gamma_a + \gamma_b + k\gamma_{D0}$	1
$-\gamma_a - \gamma_b + (k+1)\gamma_{D0}$	1
$\gamma_1 + \gamma_2 + \gamma_3 + \gamma_4 + k\gamma_{D0}$	$y + y^{-1}$
$-\gamma_1 - \gamma_2 - \gamma_3 - \gamma_4 + (k+1)\gamma_{D0}$	$y + y^{-1}$
$(k+1)\gamma_{D0}$	$y^3 + 6y + y^{-1}$

(1.11)

with  $k \geq 0$  and

$$\begin{aligned} r \in \{1, 2, 3, 4\}, \quad s \in \{5, 6, 7, 8\} \\ (a, b) \in \{(1, 3), (1, 4), (2, 3), (2, 4), (5, 7), (5, 8), (6, 7), (6, 8)\} \end{aligned} \quad (1.12)$$

where  $\gamma_{D0} = \sum_{i=1}^8 \gamma_i$ , and again the spectrum also includes the respective antiparticles obtained by sending  $\gamma \rightarrow -\gamma$ . This spectrum consists of two copies of the weakly coupled spectrum of  $SU(2)$  SQCD with two fundamental hypermultiplets in 4d [5], with the extra KK towers in lower part of the table. Again, this differs from what could be expected from the low-energy gauge theory phase of this SCFT, which is five-dimensional  $N_f = 4$   $SU(2)$  gauge theory. As for local  $\mathbb{F}_0$  and  $dP_3$ , we observe once again that the spectrum is organized into towers, over  $\gamma_r, \gamma_s$  and  $\gamma_t, \gamma_a + \gamma_b, \gamma_1 + \gamma_2 + \gamma_3 + \gamma_4, \gamma_{D0}$  with steps  $\gamma_1 + \gamma_2 + \gamma_3 + \gamma_4, \gamma_5 + \gamma_6 + \gamma_7 + \gamma_8$  and  $\gamma_{D0}$ , in a way that is reminiscent of “peacock patterns” [46].

A byproduct of these results are new and highly nontrivial wall-crossing identities. For

example, for local  $\mathbb{F}_0$  we find

$$\begin{aligned}
& \prod_{k \geq 0}^{\nearrow} \Phi(X_{\gamma_1+k(\gamma_1+\gamma_2)}) \Phi(X_{\gamma_3+k(\gamma_3+\gamma_4)}) \\
& \quad \times \prod_{s=\pm 1} \prod_{k \geq 0} \Phi((-y)^s X_{\gamma_1+\gamma_2+k\gamma_{D0}})^{-1} \cdot \Phi((-y)^s X_{\gamma_3+\gamma_4+k\gamma_{D0}})^{-1} \\
& \quad \times \prod_{k \geq 0}^{\searrow} \Phi(X_{\gamma_2+k(\gamma_1+\gamma_2)}) \Phi(X_{\gamma_4+k(\gamma_3+\gamma_4)}) \\
& = \prod_{k \geq 0}^{\nearrow} \Phi(X_{\gamma_2+k(\gamma_2+\gamma_3)}) \Phi(X_{\gamma_4+k(\gamma_4+\gamma_1)}) \\
& \quad \times \prod_{s=\pm 1} \prod_{k \geq 0} \Phi((-y)^s X_{\gamma_4+\gamma_1+k\gamma_{D0}})^{-1} \cdot \Phi((-y)^s X_{\gamma_2+\gamma_3+k\gamma_{D0}})^{-1} \\
& \quad \times \prod_{k \geq 0}^{\searrow} \Phi(X_{\gamma_3+k(\gamma_2+\gamma_3)}) \Phi(X_{\gamma_1+k(\gamma_4+\gamma_1)}).
\end{aligned} \tag{1.13}$$

Here

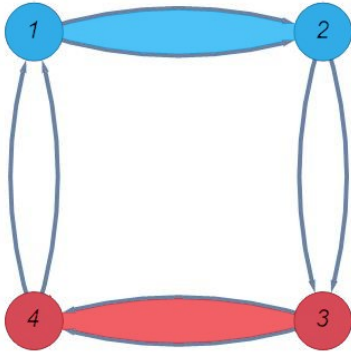
$$\Phi(x) = (-yx; y^2)_\infty^{-1}, \quad (x; y)_\infty \equiv \prod_{n=1}^{\infty} (1 - y^n x), \tag{1.14}$$

and  $\gamma_1, \dots, \gamma_4$  are generators of the charge lattice  $\Gamma \simeq \mathbb{Z}^4$ ,  $X_\gamma$  are quantum-torus algebra variables with product twisted by the DSZ pairing  $X_\gamma X_{\gamma'} = y^{\langle \gamma, \gamma' \rangle} X_{\gamma+\gamma'}$ , and  $\nearrow$  ( $\searrow$ ) denotes increasing (decreasing) values of  $k$  from left to right. The analogues of this identity for the case of  $dP_3$ ,  $dP_5$  are contained in equations (4.79) and (4.106) respectively.

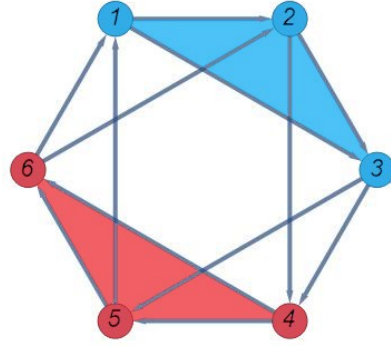
## Contents of the paper

This paper is structured as follows. We introduce the necessary background in Section 2; after recalling the notion of BPS quiver and mutation, we define what is meant by a collimation chamber, giving the example of pure  $SU(2)$  super Yang-Mills and  $\mathcal{N} = 2^*$  theory in 4d. After this, we introduce the KS invariant  $\mathbb{U}$ , and discuss how it can be constrained by using permutation symmetries of the quiver. In section 3 we review how the lattice of BPS charges can be identified with the even-dimensional cohomology of the local Calabi-Yau, and for rank-1 SCFTs the sublattice of flavor charges is organized as an affine root lattice of type  $E_n^{(1)}$ . We then discuss how to extend to the whole BPS charge lattice of the local Calabi-Yau the action of the Cremona isometries of the del Pezzo surface, which are famously related to an action of the affine Weyl group on the  $E_n^{(1)}$  root lattice. We identify this isometry group with the group of self-dualities of the five-dimensional theory, and formulate in section 3.4 a set of criteria to associate a collimation chamber to an affine Weyl translation. In section 4 we test our ideas in three specific examples, that of local  $\mathbb{F}_0$ , local  $dP_3$  and local  $dP_5$ , for all of which we find appropriate collimation chambers and conjectural expressions for the wall-crossing invariants, leading to novel wall-crossing identities.

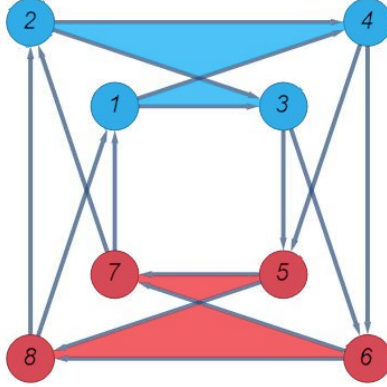




(a) Four-dimensional subquivers for the flow  $T_1$  of  $\mathbb{F}_0$ . The towers (4.16) are two copies of the dyons for 4d  $SU(2)$  pure SYM, with additional  $D0$  towers over the 4d vector multiplets.



(b) Four-dimensional subquivers for the flow  $T_1$  of  $dP_3$ . The towers (4.56) are two copies of the dyons for 4d  $SU(2)$  SYM with  $N_f = 1$ , with the addition of  $D0$  towers over the 4d quarks and vector multiplets.



(c) Four-dimensional subquivers for the flow  $T_5$  of  $dP_5$ . The towers (4.88) are two copies of the dyons for 4d  $SU(2)$  SYM with  $N_f = 2$ , with the addition of  $D0$  towers over the 4d quarks and vector multiplets.

**Figure 1**

## Acknowledgements

We thank Sibasish Banerjee, Giulio Bonelli, Michele Cirafici, Cyril Closset, Michele Del Zotto, Alba Grassi, Boris Pioline, Mauricio Romo and Alessandro Tanzini for discussions and correspondence. The work of FDM is supported by the NSERC through a CRM-ISM postdoctoral fellowship. The work of PL is supported by NCCR SwissMAP, funded by the Swiss National Science Foundation.

## 2 Symmetry constraints on wall-crossing invariants

### 2.1 Quivers, stability conditions and BPS states

The notion of moduli space of stability conditions is a fundamental piece of data in the description of the spectrum of BPS states, in the context of SUSY gauge theories, string theory, and mathematics. In this paper we focus mainly on BPS states described by quivers, for which a notion of stability condition is provided by King's  $\theta$ -stability [47].<sup>6</sup>

Recall that a quiver  $Q$  is an oriented graph, consisting of a set of  $m$  vertices  $Q_0$  and a set of oriented edges  $Q_1$ . In what follows we will restrict to quivers without loops (arrows from a node to itself) or 2-cycles (i.e. where a pair of nodes is connected by at least one arrow in each direction). In this case the structure of  $(Q_0, Q_1)$  may be encoded by an antisymmetric adjacency matrix  $B_{ij} = -B_{ji}$  whose non-negative entries are the number of arrows from node  $j$  to node  $i$ .<sup>7</sup> A quiver representation of dimension  $\vec{d} = (d_1, \dots, d_m)$  is a collection of vector spaces with dimension  $\dim V_i = d_i$ , and linear maps  $\phi_a \in \text{Hom}(V_i, V_j)$  for each arrow  $a : i \rightarrow j$ . The stability data for the representation  $R_{\vec{d}} = (\{V_i\}, \{\phi_a\})$  is a collection of reals  $\theta_i$  for each  $i \in Q_0$ . The role of  $\theta_i$  in physics is that of Fayet-Iliopoulos couplings for an  $\mathcal{N} = 4$  quantum mechanics associated to  $R_{\vec{d}}$  in the Higgs branch regime, see [4, 28, 31] for details. This quantum mechanics describes the worldvolume dynamics of a collection of fractional branes with charges  $\gamma_i$  for  $i = 1, \dots, m$ . Let  $\Gamma = \oplus_i \gamma_i \mathbb{Z}$  be the charge lattice generated by nodes of the quiver, and recall the central charge is a linear function on  $\Gamma$

$$Z \in \text{Hom}(\Gamma, \mathbb{C}). \quad (2.1)$$

In a regime when central charges are nearly aligned, the FI couplings are related to the central charges as

$$\theta_i = |Z_{\gamma_i}| (\arg Z_{\gamma_i} - \arg Z_{\gamma}) \quad (2.2)$$

where  $\gamma = \sum_i d_i \gamma_i$  is the total charge of  $R_{\vec{d}}$ , and  $Z_{\gamma} \in \mathbb{C}$  is the central charge of a BPS state with charge  $\gamma$ . The Dirac-Schwinger-Zwanziger pairing of basic charges is encoded by the quiver adjacency matrix

$$\langle \gamma_i, \gamma_j \rangle = B_{ij}. \quad (2.3)$$

Thanks to linearity of central charge as a function of  $\gamma$ , the relation (2.2) allows to trade  $\theta_i$  for  $Z_{\gamma_i}$  in discussing stability conditions.

The values of FI couplings  $\theta_i$ , or equivalently central charges  $Z_{\gamma_i}$ , determine whether a representation  $R_{\vec{d}}$  is (semi-)stable or not. In the case when (semi-)stable representations with given dimension  $\vec{d}$  exist, we denote by  $\Omega(\gamma, y)$  the shifted Poincaré polynomial of the moduli space of such representations modulo gauge equivalence, where  $\gamma = \sum_i d_i \gamma_i$ .<sup>8</sup> In

<sup>6</sup>All quivers considered in this paper arise in the study of D-branes on local Calabi-Yau threefolds. See e.g. [48–52] for further work on the relation to  $\Pi$ -stability and Bridgeland stability.

<sup>7</sup>This convention follows [4] and other papers in the physics literature. It is opposite to the convention often used in mathematics, where  $B_{ij} > 0$  would encode the number of arrows  $i \rightarrow j$ .

<sup>8</sup>The Poincaré polynomial is defined with respect to compactly supported de Rham cohomology of the moduli space  $\mathcal{M}_{\vec{d}}(\vec{\theta})$  of (semi-)stable quiver representations. This is the appropriate definition for counting BPS states in string theory, but differs from the one that would be appropriate to discuss BPS states in

physics  $\Omega(\gamma, y)$  coincides with (an uplift of) the Protected Spin Character introduced in [55], which counts BPS states with different spin. A convenient pictorial description of the BPS spectrum for a given choice of stability data is provided by *ray diagrams*, where each BPS state is represented by a vector in the  $Z$ -plane, see Figure 4.

**Mutations.** Sometimes it is useful to consider how the quiver description of BPS states changes with different choices of positive half-plane (corresponding to  $\text{Re}Z > 0$  in Figure 4). If we keep the stability condition fixed, the BPS rays do not move. However the ray diagram changes whenever the choice of half-plane is tilted so that one of the rays exits from one side or the other (the CPT-conjugate ray with  $Z_\gamma \rightarrow -Z_\gamma$  enters on the other side). The quiver description of the BPS spectrum also changes, by a left or right mutation of  $Q$  [4, 5, 33].

Note that the BPS rays which are closest to either half-boundary of the positive  $Z$  half-plane always correspond to central charges of some of the quiver nodes. When the half-plane is tilted clockwise, so that a single ray exists, the quiver changes by a mutation on the node corresponding to the exiting ray. A mutation  $\mu_k$ , acting on the node  $k$  of  $Q$ , produces a new BPS quiver  $Q'$  with adjacency matrix  $B'_{ij}$  defined as follows

$$B'_{ij} = \begin{cases} -B_{ij}, & i = k \text{ or } j = k, \\ B_{ij} + \frac{B_{ik}|B_{kj}| + B_{kj}|B_{ik}|}{2}, & \end{cases} \quad (2.4)$$

At the same time, the charge vectors  $\{\gamma_i\}$  labeling nodes of  $Q$  also change to new labels  $\{\gamma'_i\}$  for the nodes of  $Q'$  as follows

$$\mu_k(\gamma_j) = \begin{cases} -\gamma_j, & j = k, \\ \gamma_j + [B_{jk}]_+ \gamma_k, & \text{otherwise.} \end{cases} \quad (2.5)$$

If the half-plane is instead rotated counterclockwise, the mutation takes the form

$$\widetilde{\mu}_k(\gamma_j) = \begin{cases} -\gamma_j, & j = k, \\ \gamma_j + [-B_{jk}]_+ \gamma_k, & \text{otherwise.} \end{cases} \quad (2.6)$$

The simultaneous changes in  $B_{ij}$  and labels of nodes are compatible, they preserve the property (2.3).

## 2.2 Collimation chambers

In this work we focus on a specific class of stability conditions, which we name *collimation chambers*. The essential property of collimation chambers is that central charges of BPS states only accumulate along  $\mathbb{R}^\pm e^{i\vartheta_0}$ , if at all. For quivers of toric CY threefolds the real ray  $\vartheta_0 = 0$  is canonically an accumulation ray, since the BPS spectrum always features towers of D0 branes with central charge  $Z_{nD0} = n2\pi/R$  for  $n \in \mathbb{Z} \setminus \{0\}$ , where  $R$  is the radius of the M-theory circle. An equivalent definition of collimation chambers, at least in

---

the geometrically engineered gauge theory. For the latter, the appropriate notion is  $L^2$  cohomology, which has the property of respecting Poincaré symmetry. See [22, 53, 54] for details.



**Figure 2:**  $K_2$ : BPS quiver for 4d pure  $SU(2)$  super Yang-Mills.

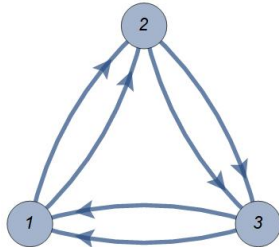


**Figure 3:**  $M_2$ : BPS quiver for the  $SU(2)$   $\mathcal{N} = 2^*$  theory

all examples we considered, is that these are stability conditions for which the only BPS states with  $Z_\gamma \notin \mathbb{R}$  are hypermultiplets, i.e. their BPS index is  $\Omega(\gamma) = 1$ .

The most basic example of a collimation chamber with at least one accumulation ray appears for the Kronecker quiver  $K_2$  with  $\langle \gamma_1, \gamma_2 \rangle = 2$  shown in Figure 2. For stability conditions within the chamber

$$\mathcal{C}_1[K_2] : \quad \arg Z_{\gamma_2} > \arg Z_{\gamma_1} \tag{2.7}$$

the ray diagram is the one of Figure 4a. This is the celebrated weak-coupling spectrum of 4d  $\mathcal{N} = 2$  super Yang-Mills theory obtained by Seiberg and Witten [56].

Another example of collimation chamber arises for the Markov quiver  $M_2$  with  $\langle \gamma_i, \gamma_{i-1} \rangle = 2$  shown in Figure 3. The ray diagram for this chamber is shown in Figure 4b, and corresponds to the chamber

$$\mathcal{C}_1[M_2] : \quad \arg Z_{\gamma_1} > \arg Z_{\gamma_3} = \arg(Z_{\gamma_1 + \gamma_2}) > \arg Z_{\gamma_2} . \tag{2.8}$$

This chamber was studied in unpublished joint work by Greg Moore and the second-named author, and was used to obtain a closed-form description of the BPS spectrum of  $\mathcal{N} = 2^*$  super Yang-Mills theory [25, 57]. The  $M_2$  quiver has two more collimation chambers  $\mathcal{C}_2[M_2], \mathcal{C}_3[M_2]$  related by cyclic permutations of the central charges in (2.8).

The Markov example is especially interesting, because it turns out that the spectrum of  $\mathcal{N} = 2^*$  theory is generically very intricate, featuring infinitely many accumulation rays. The only known exception is precisely the collimation chamber of Figure 4b (or its  $\mathbb{Z}_3$  images  $\mathcal{C}_2, \mathcal{C}_3$ ), where the BPS spectrum admits a simple exact description. In fact this correlation between collimation chambers and nice BPS spectra turns out to generalize to (at least certain) quivers of toric Calabi-Yau threefolds, suggesting that closed-form exact descriptions of the spectrum can be obtained by studying such chambers. In the rest of this paper we explore and realize this idea for a few selected examples.

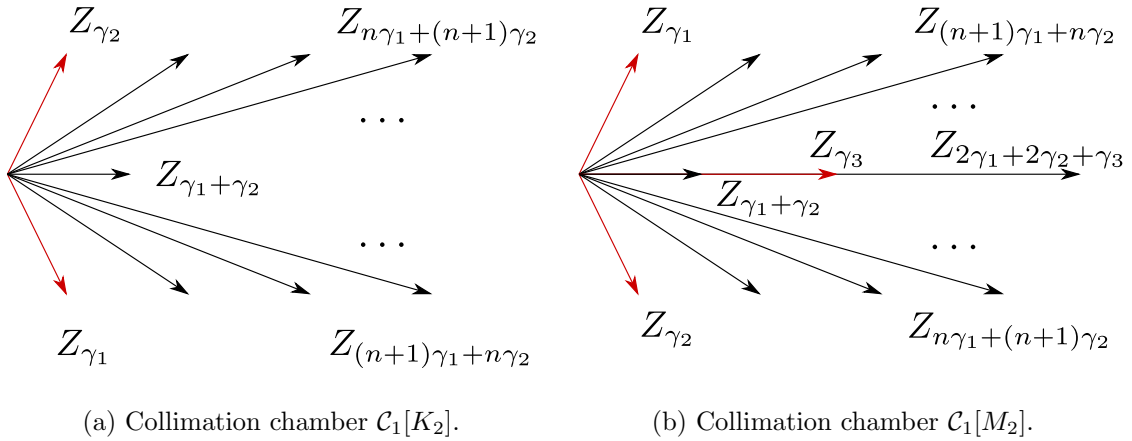


**Figure 4:** Ray diagrams of collimation chambers.

### 2.3 The wall-crossing invariant $\mathbb{U}$

The moduli space of stability conditions has a wall-and-chamber structure, with different BPS spectra in different chambers. Jumps of the spectrum are described by the wall-crossing formulae [11, 12]. We will adopt here the framework of Kontsevich and Soibelman, whose formula can be stated as a conservation law for a certain invariant  $\mathbb{U}$  built from the BPS spectrum.

Assume  $\text{Re}Z_{\gamma_i} > 0, \forall i \in Q_0$ , we shall refer to BPS particles as those BPS states whose central charge lies in the right-half of the  $Z$ -plane, and anti-particles as those in the other half<sup>9</sup>. Let  $\Gamma = \oplus_i \gamma_i \mathbb{Z}$  denote the lattice of charges generated by quiver nodes, and consider the quantum torus algebra of formal variables  $X_\gamma$  obeying

$$X_\gamma X_{\gamma'} = y^{\langle \gamma, \gamma' \rangle} X_{\gamma + \gamma'}. \quad (2.9)$$

The Kontsevich-Soibelman invariant of wall-crossing is a product of quantum dilogarithms

$$\mathbb{U} = \prod_{\gamma \in \Gamma_+} \prod_{m \in \mathbb{Z}} \Phi((-y)^m X_\gamma)^{a_m(\gamma)} \quad (2.10)$$

where

- $\Gamma_+ = \{\gamma \in \Gamma, \text{Re}Z_\gamma > 0\}$
- the ordering  $\curvearrowright$  is by increasing  $\arg(Z_\gamma)$  to the left
- $\Omega(\gamma, y) = \sum_m (-y)^m a_m(\gamma)$  is the Protected Spin Character [55], which recovers the BPS index for  $y \rightarrow -1$ .
- $\Phi(x) = (-yx; y^2)_\infty^{-1} = \prod_{s \geq 0} (1 + y^{2s+1}x)^{-1}$

<sup>9</sup>We make this choice of half-plane instead of the more traditional upper half-plane so as to have the D0-brane central charge, which is real and positive, at the center of the domain.

- $m \in \mathbb{Z}$  is the eigenvalue of  $2J_3$ , a Cartan generator of the rotation group in three dimensions<sup>10</sup>

When the stability condition belongs to a collimation chamber, the wall-crossing invariant takes the form

$$\mathbb{U} = \mathbb{U}(\angle^+) \cdot \mathbb{U}(\mathbb{R}^+) \cdot \mathbb{U}(\angle^-) \quad (2.11)$$

where  $\angle^+$  and  $\angle^-$  correspond respectively to angular sectors  $0 < \arg Z < \pi/2$  and  $-\pi/2 \leq \arg Z < 0$ . The terms  $\mathbb{U}(\angle^\pm)$  contain only (possibly countably infinitely many) hypermultiplet factors  $\Phi(X_\gamma)$ .<sup>11</sup> A consequence of this, is that in collimations chambers it is straightforward to compute  $\mathbb{U}(\angle^\pm)$  by standard techniques based on quiver mutations [4, 5, 17]. The only nontrivial task is the computation of  $\mathbb{U}(\mathbb{R}^+)$ .

**Remark 1.** *For the BPS spectrum to be well-defined in a collimation chamber, one must ensure that the marginal stability condition is not verified. This implies that for any pair of  $\gamma, \gamma' \in \Gamma$  such that  $Z_\gamma/Z_{\gamma'}$  (either on the real ray, or away from it) their pairing vanishes  $\langle \gamma, \gamma' \rangle = 0$ . However, this requirement could also be slightly relaxed. For example, if one is willing to forgo a factorization of  $\mathbb{U}(\mathbb{R}^+)$  into quantum dilogarithms, then one may still make sense of this factor as a formal series in  $X_\gamma$  even if the states with real central charge are at marginal stability with respect to each other.*

## 2.4 Quiver permutation symmetry

Before proceeding with the task of determining  $\mathbb{U}(\mathbb{R}^+)$ , we take a brief technical detour to introduce the notion of permutation symmetries of a quiver.

Let  $\Pi_Q$  be the group of permutations acting on the labels of  $Q_0$  which preserves the structure of the quiver. This is the subgroup of  $S_{|Q_0|}$  of elements

$$\pi : \gamma_i \mapsto \gamma'_i = \gamma_{\pi(i)} \quad (2.12)$$

such that the quiver  $(Q, \{\gamma'_i\})$  is identical to the original one  $(Q, \{\gamma_i\})$ . For example the  $M_2$  quiver of Figure 3 has a permutation symmetry  $\Pi_{M_2} \simeq \mathbb{Z}_3$ , acting as  $\gamma_i \mapsto \gamma_{i+1 \bmod 3}$ . An example of a quiver with trivial symmetry group is the Kronecker quiver (2).

Later we will encounter a more general definition of quiver symmetries, involving mutations. The group of  $\Pi_Q$  is a subgroup of the full automorphism group  $\text{Aut}_Q$  of the quiver, whose definition will be introduced in section 3.3). For later convenience, we highlight a few important features of mutations and permutations. Here we simply state these as (partly obvious) facts, their scope will become more clear with examples below.

- A mutation cannot change the stability condition. A permutation can. The action of  $\pi \in \Pi_Q$  restricts to permutations of collimation chambers  $\mathcal{C}_\alpha \mapsto \mathcal{C}_{\pi(\alpha)}$ . This action is generically not faithful. For an example we refer to Observation 1 for local  $\mathbb{F}_0$ .

<sup>10</sup>A standard physical realization of BPS quivers we study below in Section (4) is M-theory on a CY threefold  $X$  times  $S^1 \times \mathbb{R}^4$ . In this setup the quiver describes the spectrum of M2 and M5 branes wrapping along  $\mathbb{R} \subset \mathbb{R}^4$ , breaking  $\mathfrak{so}(4)$  to  $\mathfrak{so}(3)$ .

<sup>11</sup>This is based on the alternative characterization of collimation chambers mentioned in Section 2.2.

- Stability conditions related by a permutation are always connected by a continuous path along which no BPS ray exits the positive half-plane of central charges (in our case, this is the half-plane  $\text{Re}Z_\gamma \geq 0$ ). For an example see Observation 2 for local  $\mathbb{F}_0$ .
- A mutation changes the choice of positive half-plane of central charges by tilting it (until the BPS ray of the mutant node exists the half-plane [4]). A permutation does not.
- The group  $\Pi_Q$  isn't preserved by mutations, because mutations generically change the structure of a quiver, hence its automorphism group. We will work with a fixed representative  $Q$  in the mutation class  $[Q]$ , and consider its symmetry group  $\Pi_Q$ .

## 2.5 Constraining $\mathbb{U}$

The outstanding task of computing  $\mathbb{U}(\mathbb{R}^+)$  in a collimation chamber can be achieved by taking advantage of the permutation symmetry of a quiver  $Q$ , whenever  $\Pi_Q$  is nontrivial. A prototypical example is the  $\mathbb{Z}_4$  symmetry of the BPS quiver of local  $\mathbb{F}_0$  in Figure 6. In this case, it was shown in [41] that constraints from this symmetry are strong enough to determine  $\mathbb{U}(\mathbb{R}^+)$ .<sup>12</sup> Here we review the basic idea, and explain how it generalizes to other quivers with nontrivial symmetries.

When a labeled quiver  $(Q, \{\gamma_i\})$  has a nontrivial permutation symmetry  $\Pi_Q$ , this imposes constraints on the wall-crossing invariant  $\mathbb{U}$ . To illustrate this, let us write the latter as a formal series in  $X_\gamma$

$$\mathbb{U} = \sum_{\gamma \in \Gamma_+} u_\gamma X_\gamma \quad (2.13)$$

where coefficients  $u_\gamma$  are Laurent polynomials in  $y$  with integer coefficients. Acting with  $\pi$  induces a permutation of the  $\gamma_i$ , which induces a relabeling of formal variables  $X_\gamma$

$$\mathbb{U} \xrightarrow{\pi} \mathbb{U}' = \sum_{\gamma} u_\gamma X_{\pi(\gamma)} = \sum_{\gamma} u_{\pi^{-1}(\gamma)} X_\gamma = \sum_{\gamma} u'_\gamma X_\gamma \quad (2.14)$$

where we used the fact that  $\gamma \in \Gamma_+ \leftrightarrow \pi(\gamma) \in \Gamma_+$ .<sup>13</sup>

Next, recall from Section 2.4 that the symmetry  $\pi$  may change the stability condition by permuting the central charges associated to the nodes, but the new configuration of central charges is connected to the old one by a smooth motion in the moduli space of  $\{Z_{\gamma_i}\} \simeq \mathbb{C}^{Q_0}$  throughout which no rays exit or enter the half-plane  $\text{Re}Z > 0$ . This implies that  $\mathbb{U}' = \mathbb{U}$  by wall-crossing invariance, and leads to the non-trivial constraint

$$u_{\pi(\gamma)} = u_\gamma. \quad (2.15)$$

Taken alone, these constraints are generically too weak to fully determine  $\mathbb{U}$  itself. But in a collimation chamber we can factorize  $\mathbb{U}$  as in (2.11) into  $\mathbb{U}(\angle^\pm)$  and  $\mathbb{U}(\mathbb{R}^+)$ . As

<sup>12</sup>More precisely, up to factors involving pure-flavor states, such as  $D0$  branes in this case. The reason is that wall-crossing invariance doesn't constrain these spectrum of purer-flavor states.

<sup>13</sup>Note that  $\Gamma_+ = \{\gamma \in \Gamma \mid \gamma = \sum_{i=1}^{Q_0} n_i \gamma_i, n_i \geq 0\}$ . By definition  $\Gamma_+$  is the subset of charges with  $\text{Re}Z_\gamma > 0$ , which is the quiver half-plane. It follows that any such  $\gamma$  is a non-negative integer linear combination of the charges  $\gamma_i$  associated to the vertices of  $Q$ .

mentioned previously, it is often easy to compute  $\mathbb{U}(\mathcal{L}^\pm)$  by standard techniques such as the mutation algorithm. With this input, (2.15) becomes powerful enough to determine  $\mathbb{U}(\mathbb{R}^+)$  entirely, or almost entirely (details below). If we further require  $\mathbb{U}(\mathbb{R}^+)$  to factorize into quantum dilogarithms, we typically find that symmetries determine the exponents  $\Omega(\gamma; y)$  uniquely.

Concretely, we shall often adopt a formal series expression for  $\mathbb{U}(\mathbb{R}^+)$

$$\mathbb{U}(\mathbb{R}^+) = \sum_{\gamma \in \Gamma_{\mathbb{R}^+}} c_\gamma X_\gamma \quad (2.16)$$

where  $\Gamma_{\mathbb{R}^+} = \{\gamma \in \Gamma \mid Z_\gamma \in \mathbb{R}^+\}$  and  $c_\gamma \in \mathbb{Z}[y, y^{-1}]$ . We then compute the coefficients  $u_\gamma(y)$  of  $\mathbb{U}$  as a function of  $c_\gamma(y)$  through (2.11), and finally impose the symmetry equations (2.15) on the  $u_\gamma(y)$  to fix the coefficients  $c_\gamma(y)$  of  $\mathbb{U}(\mathbb{R}^+)$ . We will illustrate this in Section 4 with several examples.

### 3 Affine root lattices and stability conditions

In the previous section we discussed collimation chambers  $\mathcal{C}_\alpha$ , and explained how they can be used in conjunction with quiver permutation symmetries  $\Pi_Q$  to obtain equations for  $\mathbb{U}$  which determine the invariant. Here we discuss in more detail the larger automorphism group  $\text{Aut}_Q$  of a quiver  $Q$ , of which permutations are generically a subgroup

$$\Pi_Q \subset \text{Aut}_Q. \quad (3.1)$$

In the cases of interests to this paper,  $\text{Aut}_Q$  contains a subgroup isomorphic to the extended affine Weyl group<sup>14</sup> for the affine Lie algebra associated to  $Q$  [37, Theorem 3.1] (also see [38] for a comprehensive discussion). The affine root lattice can be naturally embedded within the charge lattice  $\Gamma$  [34]. One of the main points of this section is to illustrate how the action of affine Weyl translations on  $\Gamma$  can be used, at least in some cases, to define stability conditions corresponding to collimation chambers.

#### 3.1 Charge lattices

Affine root lattices naturally describe the flavor symmetry group of five-dimensional SCFTs, from the geometry of the Calabi-Yau threefold from which the field theory is obtained in M-theory compactification [58, 59]. In the case of rank-1 theories, the relevant geometry consists of local del Pezzos  $X = K_S$  with  $S = dP_n$   $n = 1, \dots, 8$ , together with local  $S = \mathbb{F}_0$ <sup>15</sup>. These are local Calabi-Yau threefolds defined as total space of the canonical line bundle of a surface  $S$ , obtained by blowing up  $\mathbb{P}^2$  at  $n$  points or  $\mathbb{P}^1 \times \mathbb{P}^1$  at  $n - 1$  points,  $n = 1, \dots, 8$ . The cases with  $S = dP_{0,1,2,3}$  are toric, while the others are not (although they still have many properties of toric manifolds, in particular shrinking one-cycles).

<sup>14</sup>This is defined as the semidirect product of the affine Weyl group of the Lie algebra and its outer automorphisms.

<sup>15</sup>More precisely, the local del Pezzo corresponds to a gauge theory phase, while its blowdown to the UV superconformal fixed point.



We now recall a few well-known facts about BPS states of type IIA string theory on  $X$ , see e.g. [21, 22] for recent accounts with additional details. The physical moduli space of the theory is called the “extended Coulomb branch” [60], including Coulomb moduli, mass parameters, and the D0 brane mass. This moduli space is geometrically realized by the Kähler parameters of the Calabi-Yau, parametrizing the resolution of its singularities and the volume of the only exceptional four-cycle, and by the radius of the M-theory circle.<sup>16</sup> BPS charges are Chern characters of compactly supported coherent sheaves, with values in the charge lattice<sup>17</sup>

$$\Gamma := H_{\text{cpt}}^{\text{even}} = H^0(X, \mathbb{Z}) \oplus H_{\text{cpt}}^2(X, \mathbb{Z}) \oplus H_{\text{cpt}}^4(X, \mathbb{Z}). \quad (3.2)$$

The lattice  $\Gamma$  is endowed with a skew-symmetric bilinear form  $\langle \cdot, \cdot \rangle$ , arising as the anti-symmetrized Euler form. Namely, for sheaves  $E_\gamma$  with charge  $\gamma$ , the pairing is

$$\langle E_\gamma, E_{\gamma'} \rangle := \chi(E_\gamma, E_{\gamma'}) - \chi(E_{\gamma'}, E_\gamma) \quad (3.3)$$

where

$$\chi(E_\gamma, E_{\gamma'}) = \int_S \text{ch}(E_\gamma^\vee) \text{ch}(E_{\gamma'}) \text{Td}(S) \quad (3.4)$$

where  $E^\vee$  is the dual sheaf to  $E$ , and  $\text{Td}$  denotes the Todd characteristic class. In gauge theory descriptions the pairing  $\langle \cdot, \cdot \rangle$  agrees with the Dirac-Schwinger-Zwanziger pairing (2.3), encoded in the quiver structure. Quiver nodes correspond to a choice of exceptional collection for  $S$ . For  $X = K_S$  with  $S$  a del Pezzo surface, the DSZ pairing matrix has rank two. This induces a (noncanonical) splitting of the charge lattice into flavor and gauge charges

$$\Gamma \simeq \Gamma_f \oplus \Gamma_g, \quad (3.5)$$

locally on moduli space. The flavor sublattice is characterized by the vanishing of  $\langle \cdot, \cdot \rangle$  when restricted to  $\Gamma_f \simeq \mathbb{Z}^f$ . We also note that in all examples of this class  $H_{\text{cpt}}^4 \simeq \mathbb{Z}$  is a sublattice of  $\Gamma_g \simeq \mathbb{Z}^2$ . When  $S = dP_n$ , we have  $\dim H^2(S, \mathbb{Z}) = n + 1$ . Since  $\dim H^0(X, \mathbb{Z}) = \dim H_{\text{cpt}}^4(X, \mathbb{Z}) = 1$ , these add up to  $\text{rk } \Gamma = n + 3$ . Moreover since  $\text{rk } \Gamma_g = 2$ , it follows that  $\text{rk } \Gamma_f = n + 1$ . Clearly all the interesting information about  $\Gamma$  is contained in  $H_{\text{cpt}}^2(S, \mathbb{Z})$ . We will discuss its structure in greater detail next.

---

<sup>16</sup>We slightly abuse terminology in calling this the “extended Coulomb branch”, since in [60] the M-theory circle radius is not included as a parameter of the theory. Rather the radius is just seen as setting a scale, which is then used to multiply masses to produce dimensionless Kähler parameters. In connection to 4d limits, from the viewpoint of field theory, one can consider various scalings where the radius is taken to zero, but they are equivalently described as limits in the Kähler moduli space. In a 5d theory on  $S^1 \times \mathbb{R}^4$  however, where we are interested in the moduli space parametrizing BPS central charges, it makes sense to include the M-theory radius. Its role is to set the overall scale of central charges, such a rescaling isn’t necessarily included in the parametrization by Kähler moduli, at least a priori. We thank Cyril Closset for helpful comments on this point.

<sup>17</sup>Actual charges would be defined by K-theory classes. The distinction between the two involves issues related to integrality of the charge lattice. For the purpose of this work we can safely ignore these.

### 3.2 Affine symmetry from geometry

While  $X$  is noncompact, by restricting to compactly supported sheaves we have  $H_{cpt}^2(X, \mathbb{Z}) \simeq H^2(S, \mathbb{Z})$ , and furthermore we can invoke Poincaré duality to identify

$$H_2(S, \mathbb{Z}) \simeq H^2(S, \mathbb{Z}) = \text{Pic}(S). \quad (3.6)$$

Under this identification, generators of  $H_2^{cpt}(S, \mathbb{Z})$  are mapped to divisors of  $S$  (i.e. line bundles) in  $\text{Pic}(S)$ . As observed in [61, 62], a natural basis of  $H_2^{cpt}(S, \mathbb{Z})$  is provided by homology classes of the exceptional curves  $\mathcal{L}_1, \dots, \mathcal{L}_n$  obtained by blowing up points in  $\mathbb{P}^2$ , as well as the pull-back of the hyperplane  $\mathcal{L}_0 \in \text{Pic}(\mathbb{P}^2, \mathbb{Z})$ . If we view instead  $dP_n$  as obtained by blowups on  $\mathbb{F}_0$ , for  $n \geq 1$  we can consider the basis of  $\text{Pic}(dP_n)$  given by  $\mathcal{H}_1, \mathcal{H}_2$  (which are total transforms of lines in  $\mathbb{F}_0$ ), and  $\mathcal{E}_1, \dots, \mathcal{E}_{n-1}$ , which are the exceptional classes of the blown-up points. Then

$$\text{Pic}(S) = \bigoplus_{i=0}^n \mathcal{L}_i = (\mathcal{H}_1 \oplus \mathcal{H}_2) \oplus \bigoplus_{i=1}^{n-1} \mathcal{E}_i. \quad (3.7)$$

The intersection form between the cycles is

$$\chi(\mathcal{L}_0, \mathcal{L}_0) = 1, \quad \chi(\mathcal{L}_0, \mathcal{L}_i) = 0, \quad \chi(\mathcal{L}_i, \mathcal{L}_j) = -\delta_{ij}, \quad i, j = 1, \dots, n, \quad (3.8)$$

$$\chi(\mathcal{H}_m, \mathcal{H}_k) = 1 - \delta_{km}, \quad \chi(\mathcal{H}_m, \mathcal{E}_k) = 0, \quad \chi(\mathcal{E}_m, \mathcal{E}_k) = -\delta_{mk}, \quad (3.9)$$

and the anti canonical class is

$$\mathcal{K}_S = 3\mathcal{L}_0 - \mathcal{L}_1 \cdots - \mathcal{L}_n = 2\mathcal{H}_1 + 2\mathcal{H}_2 - \mathcal{E}_1 \cdots - \mathcal{E}_{n-1}. \quad (3.10)$$

A remarkable fact about these geometries [61, 62] is that there exist a subset of  $n$  generators  $\{\alpha_i\}$  of  $\text{Pic}(dP_n)$  for which the intersection form is (minus) the Cartan matrix of the  $E_n$  algebra:

$$(\alpha_i, \alpha_j) = -C_{ij}^{(E_n)}, \quad (3.11)$$

so that  $\{\alpha_i\}$  can be regarded as the simple roots of  $E_n$ .

Together with the only generator  $\delta$  of  $H^0(X, \mathbb{Z})$ , with which they all have vanishing pairing (3.4) suitably extended to  $X$ , they generate the flavor lattice  $\Gamma_f$ . Physically  $\delta$  is identified with the D0 brane charge. This is therefore isomorphic to the root lattice  $\mathcal{Q}(\widehat{\mathfrak{g}})$  of the affine Lie algebra  $E_n^{(1)}$ , where  $\delta$  is the null root

$$\Gamma_f \simeq \mathcal{Q}(\widehat{\mathfrak{g}}). \quad (3.12)$$

The gauge charge lattice  $\Gamma_g \simeq \mathbb{Z}^2$  is instead generated by the remaining cycle in  $\text{Pic}(S)$  and by the unique generator of  $H_{cpt}^4(X, \mathbb{Z})$ .

**Remark 2.** *The DSZ pairing descends from the Euler form (3.3) by antisymmetrization, and it is trivial on  $\Gamma_f$ . The DSZ pairing plays a prominent role in the dynamics of BPS states, and their wall-crossing phenomena, and encodes the structure of the BPS quiver  $Q$ . On the other hand, the information encoded by the Euler form, which is hidden by the antisymmetrization, contains key information about the symmetries of the underlying theory embedded in the structure of  $\Gamma_f$  [61, 62]. Remarkably, information about these symmetries is not quite lost. As we will review below, they are encoded in  $\text{Aut}_Q$ .*

$$\begin{array}{cccccccc}
E_8^{(1)} & E_7^{(1)} & E_6^{(1)} & E_5^{(1)} & E_4^{(1)} & E_3^{(1)} & E_2^{(1)} & E_1^{(1)} \\
E_8^{(1)} & E_7^{(1)} & E_6^{(1)} & D_5^{(1)} & A_4^{(1)} & (A_2 + A_1)^{(1)} & (A_1 + A_1)^{(1)} & A_1^{(1)}
\end{array}$$

**Table 1:** Notation for affine exceptional algebras

### 3.3 Cremona isometries, affine translations, and $\text{Aut}_Q$

The Cremona isometries  $\text{Cr}(S)$  automorphisms of  $\text{Pic}(S)$  that preserve the intersection form, the canonical class and the semi-group of effective divisors of  $\text{Pic}(S)$  [42, 63]. Since they preserve the canonical class, they are also the automorphisms of the local del Pezzo CY manifolds (that are the total space of the canonical bundle), preserving the intersection form and the semi-group of effective divisors of the base.<sup>18</sup> It is well-known that such transformations are realized as the extended affine Weyl group  $\widetilde{W}(\widehat{\mathfrak{g}})$  acting not only on the root lattice  $\Gamma_f$ , but on the whole lattice  $\Gamma$  [38, 64].

It was shown in [37, 38] that  $\text{Aut}_Q$  contains a subgroup isomorphic to the extended affine Weyl group  $\widetilde{W}(\widehat{\mathfrak{g}})$  for all quivers of del Pezzo surfaces up to  $dP_8$  and of  $\mathbb{F}_0$

$$\text{Aut}_Q \supseteq \widetilde{W}(\widehat{\mathfrak{g}}). \quad (3.13)$$

Thus elements  $\text{Aut}_Q$ , which are realized by specific sequences of mutations, permutations and inversion, provide a realization of the Cremona group of  $dP_n$  on the associated BPS charge lattice  $\Gamma$ . Since  $\text{Aut}_Q$  preserves the form of the quiver, it may be regarded as the *self-duality* group of the quiver quantum mechanics.

When extending the representation of  $\widetilde{W}(\widehat{\mathfrak{g}})$  from  $\Gamma_f$ , where it is naturally defined, to  $\Gamma$ , there are subtleties to deal with: in order to have a proper representation of  $\widetilde{W}(\widehat{\mathfrak{g}})$  on  $\Gamma$ , it seems necessary to use transformations that include both clockwise and anticlockwise mutations, as was done in [38]. However this is unnatural from a physical point of view: we require that the action must include only left (or only right) mutations, in keeping with our goal of connecting to tilting induced by stability conditions as in the mutation method of [4, 5, 33, 65]. Instead, we will adopt a realization of  $\widetilde{W}(\widehat{\mathfrak{g}})$  involving only left mutations as in [37].<sup>19</sup> This will result in an action on  $\Gamma$  which is generally *not* a proper representation of  $\widetilde{W}(\widehat{\mathfrak{g}})$ , but restricts to a proper representation on the root lattice  $\Gamma_f$  (on  $\Gamma$  we have a representation “modulo seed isomorphisms” [38, 64]). Recall that affine Weyl groups have the following decomposition into reflections and translations

$$W(\widehat{\mathfrak{g}}) = W(\mathfrak{g}) \ltimes \mathcal{T}(\widehat{\mathfrak{g}}). \quad (3.14)$$

<sup>18</sup>As we have reviewed above, from the point of view of the local Calabi-Yau, in order to get the affine root lattice it is necessary to consider not just  $\text{Pic}(S)$ , but also  $H^0(X)$ , which contains the null root. However, the del Pezzo contains all the information about the local Calabi-Yau through its canonical divisor. Consequently, in the literature on q-Painlevé equations, where affine root lattices are traditionally seen as arising from del Pezzo surfaces, the null root is identified with the canonical divisor of  $dP_9$  (note that equation (3.10) implies that  $\chi(\mathcal{K}_{dP_9}, \mathcal{K}_{dP_9}) = 0$ ), which is then mapped to lower del Pezzos through a blowdown procedure [42].

<sup>19</sup>Clearly, it would be important to determine to what extent the condition of using only left (or right) mutations determines *uniquely* the realization of  $\widetilde{W}(\widehat{\mathfrak{g}}) \subset \text{Aut}_Q$ .

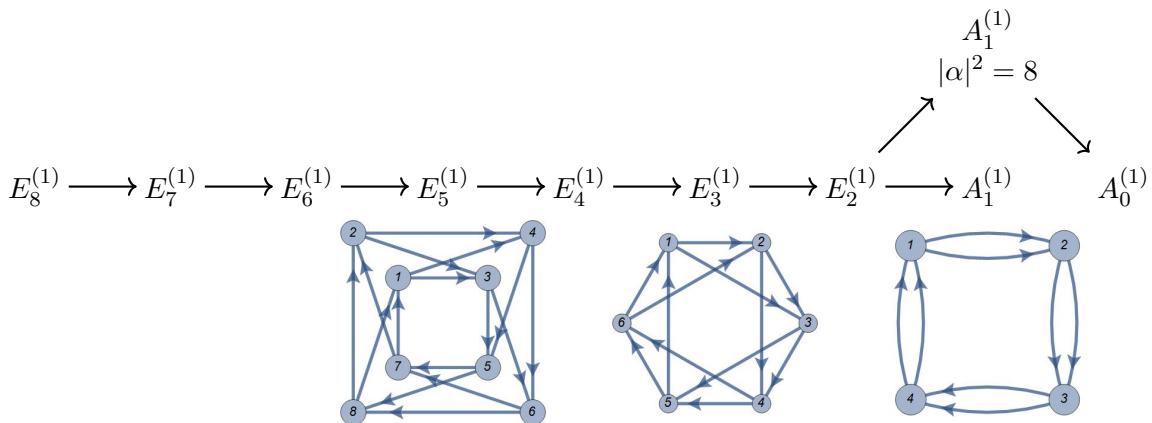


**Figure 5:** Symmetry algebra of 5d SCFTs (or symmetry type of q-Painlevé equations) with BPS quivers for local  $dP_5, dP_3, \mathbb{F}_0$ .

In the context of discrete Painlevé equations the group  $\mathcal{T}(\widehat{\mathfrak{g}})$  corresponds to the flow described by the equations themselves, while other elements of  $\widehat{W}(\widehat{\mathfrak{g}})$  act as symmetries of the equation. Following the general philosophy of [34], we want to study the action of affine translations on the lattice  $\Gamma$  of BPS charges, to study the BPS spectral problem. To this end, we recall the quiver description of BPS states reviewed in Section 2.1. For general toric geometries, BPS quivers can be determined by resorting to brane tiling techniques (see [66] for a recent review). Other options include: local mirror symmetry [62], studying calibrated one-cycles on the mirror curve [13, 15, 16, 67], directly deriving the adjacency matrix directly from  $\text{Pic}(S)$  as in [38], and the approach based on the geometry of loop groups of [36]. We collect the relevant quivers in Figure 5.

Having identified the relevant BPS quivers (labeled by  $\gamma_i$ ), the next step is to explain how these are related the affine Weyl group action on  $\Gamma$ . Recall the definition of mutations from section 2.1. In addition to this we'll need another important transformation, called inversion and denoted by  $\iota$ . This operation reverses the orientation of all arrows in  $Q$ , and flips the signs of all label charges

$$\iota(B) = -B, \quad \iota(\gamma_i) = -\gamma_i. \quad (3.15)$$

The automorphism group  $\text{Aut}_Q$  of the quiver  $Q$  consists of sequences of mutations, permutations of the nodes, and inversions, that preserve the quiver  $Q$ .

As already mentioned, affine Weyl translations (3.14) have a distinguished role through their appearance as time flows in the theory of discrete Painlevé equations. In general, a translation  $T \in \mathcal{T}(\widehat{\mathfrak{g}})$  acts on simple roots  $\alpha_i$  as follows [68]

$$T_{\vec{n}}(\alpha_i) = \alpha_i + n_i \delta, \quad \delta = \sum_i m_i \alpha_i, \quad \sum n_i m_i = 0, \quad (3.16)$$

for some choice of  $n_i$ . For  $dP_n$  there are  $n$  solutions to the last equation above, correspond-

ing to the existence of  $n$  independent flows

$$\mathrm{rk} \mathcal{T}(E_n^{(1)}) = n. \quad (3.17)$$

The action of a generic translation can be obtained as a sequence of elementary reflections on the root lattice, possibly followed by a permutation of the roots. See [68, Section 3.2] for a convenient way to compute the translation in terms of reflections.

Once a translation  $T \in \mathcal{T}(E_n^{(1)})$  is realized as an element of  $\mathrm{Aut}_Q$ , its action gets extended from  $\Gamma_f$  to the whole  $\Gamma$ . The key data encoding this extended action is a collection of *limiting rays* in  $\Gamma$ . A limiting ray is defined as  $\delta_j \mathbb{Z} \subset \Gamma$ , where

$$\delta_j = \lim_{k \rightarrow \infty} \frac{1}{k} T^k(\gamma_i) \quad (3.18)$$

for some charge  $\gamma_i$  labeling the  $i$ -th node of the quiver. The collection of all limiting rays is obtained by applying the above definition to all  $\gamma_i$  (some  $\gamma_i$ 's may have the same limiting ray, other maybe left invariant by translations).

### 3.4 Stability condition for local del Pezzos from affine translations

We now come to the main point of this section, namely to explain the relevance of (extended) affine Weyl group symmetries arising within the Cremona group of  $X$ , for the study of BPS states encoded by a quiver  $Q$ . As emphasized in Section 3.3, there is an important distinction between affine Weyl translations  $\mathcal{T}$  and the rest of  $\mathrm{Aut}_Q$ , which arises naturally in the study of discrete Painlevé equations. Furthermore these equations and the time evolution described by  $\mathcal{T}(\widehat{\mathfrak{g}})$  also play a role in the study of BPS spectrum of the quiver  $Q$ . In particular, [34] showed explicitly how affine translations <sup>20</sup>  $\mathcal{T}(A_1^{(1)})$  reproduce the sequence of mutations for the BPS quiver of  $\mathbb{F}_0$  discussed in [17], and conjectured that this observation should generalize to the other del Pezzo geometries by studying the action of discrete flows on the BPS charges of local  $\mathbb{F}_1$  and local  $dP_3$ .

In this paper we wish to make the above proposal more precise, identifying a relation between affine translations and certain stability conditions. Furthermore, in all examples we considered it turns out that the class of stability conditions arising from affine Weyl translations often belongs to a collimation chamber, as introduced in Section 2. This fact will allow us to compute the wall-crossing invariant order by order as outlined in Section 2.5. Our goal is to associate uniquely a collimation chamber to an appropriate Weyl translation

$$T \mapsto \mathcal{C}_T. \quad (3.19)$$

A priori it is unclear whether a Weyl translation  $T$  should correspond to a stability condition. In fact, through (3.13) a translation  $T$  may generically be realized as a sequence of mutations, permutations, and possibly certain involutions on  $Q$ . There are three basic conditions that  $T$  must satisfy, in order for (3.19) to make sense:

- (c1) There is a positive integer  $k \in \mathbb{N}$  such that  $T^k = \mu_{i_1} \dots \mu_{i_\ell}$  admits an expression involving only left mutations.

---

<sup>20</sup>More precisely, the double cover  $2 \cdot \mathcal{T}$ , see below.

(c2) There exists a configuration of  $Z_{\gamma_i} \in \mathbb{C}$  such that clockwise tilting the positive half-plane induces a sequence of mutations identical to iterations of  $(T^k)^n$  for  $n \geq 1$ .

(c3) The above configuration of central charges belongs to a collimation chamber.

If criteria (c1)-(c2) are satisfied, we can associate a stability condition to  $T$ . The third requirement is only needed to restrict to stability conditions of collimation type.

In general it is not always clear how to verify whether an affine translation  $T$  (more precisely, its realization in  $\text{Aut}_Q$ ) satisfies the above criteria. (c1) is the easiest to verify: for example if  $T$  only involves left mutations and permutations one takes  $k$  to be the order of the permutation  $\pi^k = 1$ . Then one uses  $\mu_i \pi = \pi \mu_{\pi(i)}$  to take all instances of  $\pi$  together so as to cancel them, leaving mutations only. Criteria (c2)-(c3) are more difficult to verify, and we will now outline a procedure tailored to this purpose.

We shall begin with some technical assumptions:

(a1) In the mapping (3.12), each simple root  $\alpha_i \in \mathcal{Q}(\hat{\mathfrak{g}})$  is realized as a linear combination of basic charges

$$\alpha = \sum_i c_{\alpha,i} \gamma_i \tag{3.20}$$

with nonzero coefficients only for a subset of mutually local  $\gamma_i$ .

(a2) We require that  $\langle \delta_i, \delta_j \rangle = 0$  for all charges of limiting rays of  $T$ .

(a3) There is a nontrivial sublattice whose roots are given by only mutually local charges.

If the first condition is not satisfied, we can still define a virtual stability condition, but it will not necessarily correspond to a collimation chamber. This second assumption is only technical, and we hope to be able to lift it in future work. It certainly does not hold in the four-dimensional case, see e.g. the example of the Kronecker quiver in Section 2.2. For the case of local del Pezzos, it fails for  $dP_1, dP_2, dP_4$ . We now explain the procedure that associates a collimation chamber to each affine translation.

**Procedure.** Given the above assumptions (a1)-(a3), we can now state a procedure to verify whether conditions (c2)-(c3) are verified. We shall proceed constructively, *i.e.* by stating a set of constraints on the possible configurations of  $Z_{\gamma_i}$  that would realize (c2)-(c3). Let  $\varphi_i = \arg(Z_{\gamma_i})$ , then we require

1. The D0-brane central charge is real

$$\arg(Z_\delta) = 0. \tag{3.21}$$

2. The limiting rays of  $T$  should lie on the real axis

$$\arg Z_{\delta_i} = 0 \quad \forall i. \tag{3.22}$$

Thanks to (a2), this does not correspond to a wall of marginal stability.

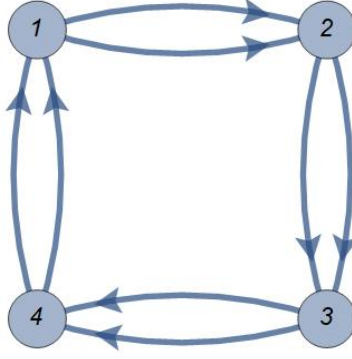


**Figure 6:** BPS quiver for local  $\mathbb{F}_0$ .

3. Since roots  $\alpha_i$  are made of mutually local charges (see (a1)), we demand that  $Z_{\gamma_i}$  of the central charges of  $\gamma_i$  contributing to (3.20) with nonzero coefficients are mutually aligned

$$\varphi_{\alpha,1} = \cdots = \varphi_{\alpha,k}. \quad (3.23)$$

In the examples that we consider this procedure constrains the  $Z_{\gamma_i}$  to the extent that it completely fixes the map (3.19).

## 4 Examples

### 4.1 $\mathbb{F}_0$

The Cremona group of  $\mathbb{F}_0$  is

$$\mathrm{Cr}(\mathbb{F}_0) = W(A_1^{(1)}) \rtimes \mathrm{Dih}_4. \quad (4.1)$$

The extended affine Weyl group

$$\widetilde{W}(A_1^{(1)}) = W(A_1^{(1)}) \rtimes \mathrm{Out}(A_1^{(1)}) \quad (4.2)$$

is a subgroup of  $\mathrm{Cr}(\mathbb{F}_0)$ , since  $\mathrm{Out}(A_1^{(1)}) \simeq \mathbb{Z}^2 \subset \mathrm{Dih}_4$  as depicted in Figure 8.

On the other hand, the full Cremona group is visible on the BPS quiver, which is depicted in Figure 6. The adjacency matrix is

$$B = \begin{pmatrix} 0 & -2 & 0 & 2 \\ 2 & 0 & -2 & 0 \\ 0 & 2 & 0 & -2 \\ -2 & 0 & 2 & 0 \end{pmatrix}. \quad (4.3)$$

The full automorphism group of  $Q$  coincides with the Cremona group [37]

$$\mathrm{Aut}_Q = \mathrm{Cr}(\mathbb{F}_0), \quad (4.4)$$

with generators

$$s_0 = (1, 3)\mu_1\mu_3, \quad s_1 = (2, 4)\mu_2\mu_4, \quad \pi = (1, 2, 3, 4), \quad \sigma = \iota(1, 3). \quad (4.5)$$

Automorphisms  $\text{Aut}_Q$  have a permutation subgroup  $\Pi_Q \simeq \mathbb{Z}_4 \subset \text{Dih}_4$ .

The rank of  $B$  is 2, therefore

$$\text{rk } \Gamma_g = \text{rk } \Gamma_f = 2. \quad (4.6)$$

A positive integral basis for  $\Gamma_f^+ = \{\gamma \in \Gamma_f, \text{Re}Z_\gamma > 0\}$  is given by

$$\gamma_{f,0} = \gamma_1 + \gamma_3, \quad \gamma_{f,1} = \gamma_2 + \gamma_4. \quad (4.7)$$

**Collimation chambers.** The moduli space of stability conditions for the quiver of Figure 6 features collimation chambers. The first one of these, found in [17], is a chamber containing the following configuration of central charges<sup>21</sup>

$$\mathcal{C}_1[\mathbb{F}_0] \supset \quad Z_{\gamma_1} = Z_{\gamma_3}, \quad Z_{\gamma_2} = Z_{\gamma_4}, \quad \arg Z_{\gamma_1} > \arg Z_{\gamma_2}, \quad Z_{\gamma_1} + Z_{\gamma_2} \in \mathbb{R}^+. \quad (4.8)$$

The authors of [17] observed that tilting the positive half-plane of central charges induces infinite sequences of left- and right-mutations, corresponding to the following towers of hypermultiplets

$$\begin{aligned} \Omega(\gamma_1 + n(\gamma_1 + \gamma_2), \mathcal{C}_1) = 1 & \quad \Omega(\gamma_2 + n(\gamma_1 + \gamma_2), \mathcal{C}_1) = 1 \\ \Omega(\gamma_3 + n(\gamma_3 + \gamma_4), \mathcal{C}_1) = 1 & \quad \Omega(\gamma_4 + n(\gamma_3 + \gamma_4), \mathcal{C}_1) = 1 \end{aligned} \quad (4.9)$$

These BPS states are those that lie off the real axis in the ray diagram of Figure 7. As  $n \rightarrow \infty$  rays accumulate towards  $Z_{\gamma_1+\gamma_2} = Z_{\gamma_3+\gamma_4} \in \mathbb{R}^+$  as required by the definition of collimation chamber.

There is also a second collimation chamber, characterized by

$$\mathcal{C}_2[\mathbb{F}_0] \supset \quad Z_{\gamma_1} = Z_{\gamma_3}, \quad Z_{\gamma_2} = Z_{\gamma_4}, \quad \arg Z_{\gamma_1} < \arg Z_{\gamma_2}, \quad Z_{\gamma_1} + Z_{\gamma_2} \in \mathbb{R}^+. \quad (4.10)$$

Again there are infinite towers of hypermultiplets accumulating towards  $\mathbb{R}^+$ , however their charges are now

$$\begin{aligned} \Omega(\gamma_1 + n(\gamma_1 + \gamma_4), \mathcal{C}_2) = 1 & \quad \Omega(\gamma_2 + n(\gamma_2 + \gamma_3), \mathcal{C}_2) = 1 \\ \Omega(\gamma_3 + n(\gamma_2 + \gamma_3), \mathcal{C}_2) = 1 & \quad \Omega(\gamma_4 + n(\gamma_1 + \gamma_4), \mathcal{C}_2) = 1. \end{aligned} \quad (4.11)$$

In either of these chambers the spectrum is not exhausted by hypermultiplets, as there are BPS states with  $Z \in \mathbb{R}_+$  that need to be determined. We'll return to this below.

Clearly, the two chambers  $\mathcal{C}_1, \mathcal{C}_2$  in (4.8) and (4.10) are related to each other by exchanging  $\{\gamma_1, \gamma_3\}$  with  $\{\gamma_2, \gamma_4\}$  (as unordered sets). This is a  $\mathbb{Z}_2$  subgroup of  $\Pi_Q$ , whose action is therefore not faithful on  $\mathcal{C}_i$ .

<sup>21</sup>Recall that by convention all  $Z_{\gamma_i}$  in this paper are understood to have positive real part. The full extent of the chamber depends on its BPS spectrum, in this case  $\mathcal{C}_1$  also contains more general configurations, such as  $Z_{\gamma_1} \neq Z_{\gamma_3}$  as long as their phases are the same.



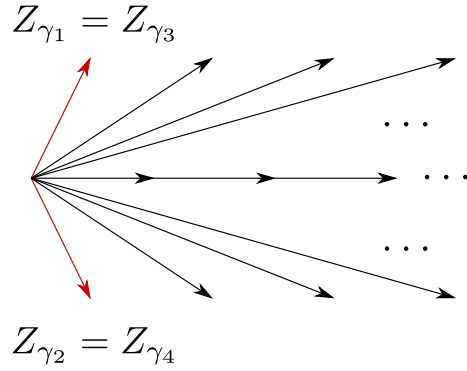


**Figure 7:** BPS ray diagram for the collimation chamber  $\mathcal{C}_1[\mathbb{F}_0]$ .

**Translations of the  $A_1^{(1)}$  lattice.** Before proceeding with the analysis of BPS states on the real ray, let us pause to explain how the collimation chambers described above could have been found by studying translations of the affine root lattice associated to the quiver. The relation between the chamber (4.8) and lattice translations was first observed by [34]. We begin by reviewing how translations of the root lattice are realized by mutations and permutations on quiver vertices.

The low-energy gauge theory phase is  $5d \mathcal{N} = 1$  pure  $SU(2)$  Yang-Mills. The isomorphism (3.12) identifies the flavor sublattice  $\Gamma_f$  with the root lattice  $\mathcal{Q}(A_1^{(1)})$ . Simple roots are identified with the generators (4.7)

$$\alpha_0 = \gamma_{f,0}, \quad \alpha_1 = \gamma_{f,1}. \quad (4.12)$$

Therefore the null root  $\delta := \sum_{i=1}^4 \gamma_i$  decomposes into  $\delta = \sum_i m_i \alpha_i$  with  $(m_0, m_1) = (1, 1)$ . Applying the general definition (3.16) of affine Weyl translations we therefore find a single translation generator  $T_1$ , defined by  $(n_0, n_1) = (1, -1)$  acting as follows on the simple roots

$$T_1^n(\vec{\alpha}) = \begin{pmatrix} \alpha_0 + n\delta \\ \alpha_1 - n\delta \end{pmatrix}. \quad (4.13)$$

Therefore in the case of local  $\mathbb{F}_0$

$$\mathcal{T}(A_1^{(1)}) \simeq \mathbb{Z}. \quad (4.14)$$

Next recall the relation (3.13) between the extended Weyl group of the affine root lattice, and quiver automorphisms. The translation subgroup  $\mathcal{T}(A_1^{(1)}) \subset \widetilde{W}(A_1^{(1)})$  is realized in  $\text{Aut}_Q$  by [37]

$$T_1 = (1, 2)(3, 4)\mu_1\mu_3 \quad (4.15)$$

Note that while the action of  $\mathcal{T}(A_1^{(1)})$  is only defined on  $\mathcal{Q}(A_1^{(1)}) \simeq \Gamma_f$ , the realization

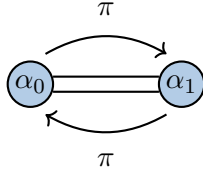


**Figure 8:**  $A_1^{(1)}$  Dynkin diagram and automorphisms

(4.15) extends to all of  $\Gamma$ , as follows

$$T_1^n(\vec{\gamma}) = \begin{pmatrix} \gamma_1 + n(\gamma_1 + \gamma_2) \\ \gamma_2 - n(\gamma_1 + \gamma_2) \\ \gamma_3 + n(\gamma_3 + \gamma_4) \\ \gamma_4 - n(\gamma_3 + \gamma_4) \end{pmatrix}. \quad (4.16)$$

As a check, when restricted to  $\gamma_{f,i}$  with  $i = 0, 1$ , the action reproduces that on  $\alpha_i$  for  $i = 0, 1$ .

The affine Weyl group contains only one set of translations (4.14). However its realization on the BPS charge lattice  $\Gamma$  isn't unique. This is because the map (4.12) can be composed with the nontrivial outer automorphism  $\pi \in \text{Out}(A_1^{(1)}) \simeq \mathbb{Z}_2$ , which exchanges the two roots

$$\pi : \quad \alpha_0 \mapsto \alpha_1, \quad \alpha_1 \mapsto \alpha_0. \quad (4.17)$$

Note that  $\text{Out}(A_1^{(1)}) \subset \widetilde{W}(A_1^{(1)})$  belongs to the extended affine Weyl group, and therefore it must admit a realization as an element of  $\text{Aut}_Q$ , by virtue of (3.13), so that  $\pi$  is really the one defined in (4.5). This means that  $\text{Out}(A_1^{(1)})$  is realized as a subgroup of quiver permutations

$$\mathbb{Z}_2 \approx \text{Out}(A_1^{(1)}) \subset \Pi_Q \approx \mathbb{Z}_4, \quad (4.18)$$

since  $\pi^4 = id$ , but  $\pi^2|_{\Gamma_f} = id$ .

Conjugation by  $\pi \in \text{Out}(A_1^{(1)})$  leads to the *same* group of affine translations, but with a *different* realization in  $\text{Aut}_Q$ . In fact the generator

$$T_2 \equiv (1, 4)(2, 3)\mu_2\mu_4 = \pi^{-1}T_1\pi. \quad (4.19)$$

acts simply as the inverse of  $T_1$  on  $\mathcal{Q}(A_1^{(1)})$

$$T_2^n(\vec{\alpha}) = \begin{pmatrix} \alpha_0 - n\delta \\ \alpha_1 + n\delta \end{pmatrix}, \quad (4.20)$$

which is the image under  $\pi$  of (4.13). However for the action on  $\Gamma$  we obtain

$$T_2^n(\vec{\gamma}) = \begin{pmatrix} \gamma_1 - n(\gamma_1 + \gamma_4) \\ \gamma_2 + n(\gamma_3 + \gamma_2) \\ \gamma_3 - n(\gamma_3 + \gamma_2) \\ \gamma_4 + n(\gamma_1 + \gamma_4) \end{pmatrix}, \quad (4.21)$$

which is the image of (4.16) under  $\pi$ .

Note that, while  $T_2 = T_1^{-1}$  on  $\mathcal{Q}(A_1^{(1)}) \simeq \Gamma_f$ , this is not so on  $\Gamma$ . This is due to the fact that we chose a realization of  $\text{Cr}(\mathbb{F}_0)$  in  $\text{Aut}_Q$  which only involves *left* mutations, as explained in Section 3.3.

**Collimation chambers from affine Weyl translations.** Having reviewed the realization of affine Weyl translations, we are now in a position to explain how these give rise to a sequence of mutations which corresponds to a stability condition. Namely, the sequence of mutations induced by lattice translations coincides with the sequence of mutations induced by tilting the positive half-plane of central charges for a certain choice of stability condition. Furthermore, this stability condition belongs to one of the collimation chambers  $\mathcal{C}_i$ .

The conditions (3.21) and (3.23) coming from the root lattice structure of  $\Gamma$  read in this case

$$\begin{cases} \varphi_1 + \varphi_2 + \varphi_3 + \varphi_4 = 0, \\ \varphi_1 = \varphi_3, \\ \varphi_2 = \varphi_4. \end{cases} \quad (4.22)$$

To discuss (3.22) we must determine the charges  $\delta_i$  of limiting rays (3.18). For the flow  $T_1$ , it is clear from (4.16) that

$$\delta_1(T_1) = \gamma_1 + \gamma_2, \quad \delta_2(T_1) = \gamma_3 + \gamma_4, \quad (4.23)$$

whereas for the flow  $T_2$  in (4.21) we have instead

$$\delta_1(T_2) = \gamma_4 + \gamma_1, \quad \delta_2(T_2) = \gamma_2 + \gamma_3. \quad (4.24)$$

In either case we find that  $Z_{\delta_i} \in \mathbb{R}^+$  thanks to (4.22). Therefore (3.22) is automatically satisfied for both flows. The general solution to (4.22) is

$$\varphi_1 = \varphi_3 = -\varphi_2 = -\varphi_4. \quad (4.25)$$

However equation (4.25) does not yet determine completely a stability condition, as it does not fully specify the phase ordering of the central charges. This last piece of information is fixed in different ways for the two flows  $T_1, T_2$ , by viewing each of them as tiltings of the positive half  $Z$ -plane. Indeed, it was observed in [34] that

$$T_1^2 = \mu_2\mu_4\mu_3\mu_1 \equiv \mathbf{m}_1 \quad T_2^2 = \mu_1\mu_3\mu_2\mu_4 \equiv \mathbf{m}_2. \quad (4.26)$$

For  $T_1$  the first mutations occur on  $\gamma_1, \gamma_3$ , implying

$$\varphi_1 = \varphi_3 > \varphi_2 = \varphi_4 = -\varphi_1. \quad (4.27)$$

The configuration of BPS rays for simple roots is shown in Figure 9a. This class of stability conditions corresponds exactly to the collimation chamber defined in (4.8)

$$\text{Stability conditions for } T_1 \equiv \text{collimation chamber } \mathcal{C}_1[\mathbb{F}_0]. \quad (4.28)$$

Conversely, the first charges mutated by the flow  $T_2$  are  $\gamma_2, \gamma_4$ , so that

$$\varphi_2 = \varphi_4 > \varphi_1 = \varphi_3 = -\varphi_2. \quad (4.29)$$

The configuration of BPS rays for simple roots is shown in Figure 9b. This class of stability conditions corresponds exactly to the collimation chamber defined in (4.10)

$$\text{Stability conditions for } T_2 \equiv \text{collimation chamber } \mathcal{C}_2[\mathbb{F}_0]. \quad (4.30)$$

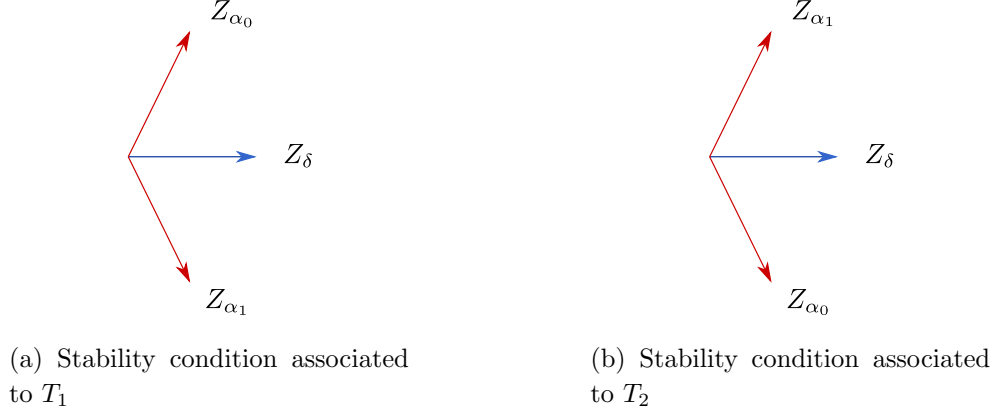


**Figure 9:** Stability conditions for  $\mathbb{F}_0$ , corresponding to  $\mathcal{C}_1[\mathbb{F}_0]$  and  $\mathcal{C}_2[\mathbb{F}_0]$  respectively.

**Wall-crossing invariant.** Let us now return to the analysis of the two collimation chambers (4.8) and (4.10), and to the computation of the wall-crossing invariant  $\mathbb{U}$ . First we make two observations

1. The chamber  $\mathcal{C}_2$  in (4.10) and the states (4.11) are related to  $\mathcal{C}_1$  in (4.8) and its BPS states (4.9) by a  $\Pi_Q \simeq \mathbb{Z}_4$  shift in charge labels  $\pi : \gamma_i \mapsto \gamma_{i+1 \bmod 4}$ . Note that  $\pi^2$  acts trivially on stability conditions, so the action of  $\Pi_Q \simeq \mathbb{Z}_4$  is not faithful on  $\{\mathcal{C}_i\}$ . Indeed, the subgroup  $\text{Out}(A_1^{(1)}) \simeq \mathbb{Z}_2$  is the one that acts faithfully on  $\{\mathcal{C}_1, \mathcal{C}_2\}$ .
2. Stability conditions (4.9) and (4.10) are connected by a path in moduli space along which no BPS rays exit the half-plane  $\text{Re}Z > 0$ . Concretely, let  $Z_{\gamma_i}^{(0)}$  be arbitrary representatives for the chamber (4.8). Then a suitable path would be

$$\begin{aligned} Z_{\gamma_1}(t) = Z_{\gamma_3}(t) &= t \cdot Z_{\gamma_1}^{(0)} + (1-t) \cdot Z_{\gamma_2}^{(0)} \\ Z_{\gamma_2}(t) = Z_{\gamma_4}(t) &= t \cdot Z_{\gamma_2}^{(0)} + (1-t) \cdot Z_{\gamma_1}^{(0)} \end{aligned} \quad t \in [0, 1] \quad (4.31)$$

Existence of a path with these properties implies that  $\mathbb{U}$  remains unchanged in moving from one stability condition to the other. Therefore

$$\mathbb{U}(\mathcal{C}_1) = \mathbb{U}(\mathcal{C}_2) \quad (4.32)$$

where each side admits a factorization of the form (2.11)

$$\mathbb{U}(\mathcal{C}_i) = \mathbb{U}(\angle^+, \mathcal{C}_i) \cdot \mathbb{U}(\mathbb{R}^+, \mathcal{C}_i) \cdot \mathbb{U}(\angle^-, \mathcal{C}_i). \quad (4.33)$$

The BPS rays off the real axis contribute, respectively in each chamber

$$\begin{aligned} \mathbb{U}(\angle^+, \mathcal{C}_1) &= \prod_{k \geq 0}^{\nearrow} \Phi(X_{\gamma_1+k(\gamma_1+\gamma_2)}) \Phi(X_{\gamma_3+k(\gamma_3+\gamma_4)}) \\ \mathbb{U}(\angle^-, \mathcal{C}_1) &= \prod_{k \geq 0}^{\searrow} \Phi(X_{\gamma_2+k(\gamma_1+\gamma_2)}) \Phi(X_{\gamma_4+k(\gamma_3+\gamma_4)}) \end{aligned} \quad (4.34)$$

and

$$\begin{aligned} \mathbb{U}(\angle^+, \mathcal{C}_2) &= \prod_{k \geq 0}^{\nearrow} \Phi(X_{\gamma_2+k(\gamma_2+\gamma_3)}) \Phi(X_{\gamma_4+k(\gamma_4+\gamma_1)}) \\ \mathbb{U}(\angle^-, \mathcal{C}_2) &= \prod_{k \geq 0}^{\searrow} \Phi(X_{\gamma_3+k(\gamma_2+\gamma_3)}) \Phi(X_{\gamma_1+k(\gamma_4+\gamma_1)}) \end{aligned} \quad (4.35)$$

where  $\nearrow$  ( $\searrow$ ) denotes increasing (decreasing) values of  $k$  to the right.

To compute  $\mathbb{U}(\mathbb{R}^+, \mathcal{C}_1)$  and  $\mathbb{U}(\mathbb{R}^+, \mathcal{C}_2)$ , consider a formal series expansion like (2.16) for each of them. Plugging these into (4.33), and imposing the equality (4.32) leads to an equation involving  $c_\gamma(\mathcal{C}_1)$  on the *l.h.s.* and  $c_\gamma(\mathcal{C}_2)$  on the *r.h.s.* Next we use the fact that factorizations  $\mathbb{U}(\mathcal{C}_1)$  and  $\mathbb{U}(\mathcal{C}_2)$  correspond to stability conditions related by a  $\mathbb{Z}_4$  relabeling of  $\gamma_i$  on quiver nodes. In particular this implies  $c_\gamma(\mathcal{C}_2) = c_{\pi^{-1}(\gamma)}(\mathcal{C}_1)$  (cf. (2.14)) and we can express both  $\mathbb{U}(\mathcal{C}_i)$  in terms of  $c_\gamma(\mathcal{C}_1) \equiv c_\gamma$  only. Wall-crossing invariance (4.32) then imposes equations on these coefficients: namely

$$\mathbb{U}(\angle^+, \mathcal{C}_1) \left( \sum_{\gamma \in \Gamma_{\mathbb{R}^+}} c_\gamma X_\gamma \right) \mathbb{U}(\angle^-, \mathcal{C}_1) = \mathbb{U}(\angle^+, \mathcal{C}_2) \left( \sum_{\gamma \in \Gamma_{\mathbb{R}^+}} c_{\pi^{-1}(\gamma)} X_\gamma \right) \mathbb{U}(\angle^-, \mathcal{C}_2). \quad (4.36)$$

This is the equation we needed to constrain  $c_\gamma$  and compute  $\mathbb{U}(\mathbb{R}^+, \mathcal{C}_i)$ . Expanding each side, this is precisely the symmetry constraint derived in (2.15). Note that this condition holds for coefficients  $u_\gamma$ , which are nontrivial functions of the  $c_\gamma$  through (2.11) and the known factors (4.34).

To solve equation (4.36) we expand each side as a series in  $X_\gamma$  and compare coefficients of the monomials. This leads to infinitely many equations which can be solved recursively by introducing a filtration in  $|\gamma| = \sum_i d_i$ . Such a procedure can be easily implemented on

a computer, and yields

$$\begin{aligned}
\mathbb{U}(\mathbb{R}^+, \mathcal{C}_1) &= 1 - \frac{1+y^2}{1-y^2} (X_{\gamma_1+\gamma_2} + X_{\gamma_3+\gamma_4}) + \frac{2y^2+y^4+y^6}{(1-y^2)(1-y^4)} (X_{2\gamma_1+2\gamma_2} + X_{2\gamma_3+2\gamma_4}) \\
&\quad - \frac{(y^4+2y^6+y^{10})}{(1-y^2)^2(1-y^6)} (X_{3\gamma_1+3\gamma_2} + X_{3\gamma_3+3\gamma_4}) \\
&\quad - \frac{(1-y^2)(1-y^4)c_{\gamma_{D0}} - 2y^2 - 3y^4 + y^6}{(1-y^2)^3} (X_{\gamma_1+\gamma_2+\gamma_{D0}} + X_{\gamma_3+\gamma_4+\gamma_{D0}}) \\
&\quad + c_{\gamma_{D0}} X_{\gamma_{D0}} + \dots
\end{aligned} \tag{4.37}$$

where we introduced the shorthand notation  $\gamma_{D0} = \sum_i \gamma_i$ .

The solution can be obtained to arbitrary orders in  $|\gamma|$ , and we find that it is compatible with the factorization

$$\mathbb{U}_0(\mathbb{R}^+, \mathcal{C}_1) = \prod_{s=\pm 1} \prod_{k \geq 0} \Phi((-y)^s X_{\gamma_1+\gamma_2+k\gamma_{D0}})^{-1} \cdot \Phi((-y)^s X_{\gamma_3+\gamma_4+k\gamma_{D0}})^{-1} \tag{4.38}$$

where  $\gamma_{D0} = \sum_{i=1}^4 \gamma_i$ . We can write this in a more suggestive way by recalling the D-brane charges associated with  $\gamma_i$  as follows

$$\mathbb{U}_0(\mathbb{R}^+, \mathcal{C}_1) = \prod_{s=\pm 1} \prod_{k \geq 0} \Phi((-y)^s X_{\gamma_1+\gamma_2+k\gamma_{D0}})^{-1} \cdot \Phi((-y)^s X_{-\gamma_1-\gamma_2+(k+1)\gamma_{D0}})^{-1}. \tag{4.39}$$

Indeed recall that  $\gamma_1 + \gamma_2$  can be identified with a D2 brane wrapping the fiber  $\mathbb{P}^1$  in  $\mathbb{F}_0$ , then the above expression makes it evident that these are towers of  $D2$ - $D0$  boundstates as well as the CPT conjugate  $\overline{D2}$ - $D0$  states which belong to the positive half  $Z$ -plane [41]. We will see this pattern arising in greater generality in other examples below.

This corresponds to a BPS spectrum along the real ray consisting of vectormultiplets

$$\Omega(\gamma_1 + \gamma_2 + n\gamma_{D0}, \mathcal{C}_1) = \Omega(-\gamma_1 - \gamma_2 + (n+1)\gamma_{D0}, \mathcal{C}_1) = y + y^{-1} \tag{4.40}$$

As observed in [41], this formula misses contributions from D0 branes, an ambiguity reflected in the fact that the coefficients  $c_{n\gamma_{D0}}$  remain undetermined. Since  $\gamma_{D0}$  has trivial pairing with any other charge  $\langle \gamma_{D0}, \gamma \rangle = 0$ , it does not participate in wall-crossing. It follows that pure D0 states cannot be fixed by our methods, which are fundamentally based on symmetries of  $Q$  in conjunction with wall-crossing invariance. The D0 contributions can be obtained with other techniques, such as exponential networks [13–16, 41] or a combination of results from Attractor Flow Tree formulae and known results about DT invariants [19, 21–23]. The expected motivic DT invariant for any number of D0 branes is [22]

$$\Omega(n\gamma_{D0}; y) = y^3 + 2y + y^{-1}. \tag{4.41}$$

The corresponding contribution to  $\mathbb{U}(\mathbb{R}^+)$  is a product of quantum dilogarithms as outlined in (2.10) *et seq.*

$$\mathbb{U}(\mathbb{R}^+, \mathcal{C}_1) = \mathbb{U}_0(\mathbb{R}^+, \mathcal{C}_1) \cdot \prod_{n \geq 1} \Phi((-y)^{-1} X_{n\gamma_{D0}})^{-1} \Phi((-y) X_{n\gamma_{D0}})^{-2} \Phi((-y)^3 X_{n\gamma_{D0}})^{-1}. \tag{4.42}$$

It is worth recalling a subtle distinction in the counting of D0 branes: the Donaldson-Thomas counting is based on compactly-supported de Rham cohomology of quiver representation varieties, while the physical counting of BPS states (pertaining e.g. to gauge theory in the context of geometric engineering) is based on the  $L^2$  cohomology [53, 69]. The latter typically contains fewer states, and leads to Poincaré-symmetric expressions for  $\Omega(\gamma, y)$  while the former does not, see [22, 54] for a discussion.

In conclusion, the spectrum we obtain for local  $\mathbb{F}_0$  in chamber  $\mathcal{C}_1$  is

$\gamma$	$\Omega(\gamma; y)$
$\gamma_1 + k(\gamma_1 + \gamma_2)$	1
$-\gamma_1 + (k+1)(\gamma_1 + \gamma_2)$	1
$\gamma_3 + k(\gamma_3 + \gamma_4)$	1
$-\gamma_3 + (k+1)(\gamma_3 + \gamma_4)$	1
$\gamma_1 + \gamma_2 + k\gamma_{D0}$	$y + y^{-1}$
$-\gamma_1 - \gamma_2 + (k+1)\gamma_{D0}$	$y + y^{-1}$
$(k+1)\gamma_{D0}$	$y^3 + 2y + y^{-1}$

(4.43)

with  $k \geq 0$ , plus the respective antiparticles obtained by sending  $\gamma \rightarrow -\gamma$ . This manifestly agrees with the explicit expression in [41], it can also be shown to agree with the generating function of stacky invariants obtained in [22].<sup>22</sup>

It should be noted that the spectrum is organized as *two* copies of the spectrum of 4d pure  $SU(2)$  SYM from the subquivers shown in Figure 18, in which the local  $\mathbb{F}_0$  quiver is divided by the time flows, with additional towers of D0 branes over the vector multiplet states.

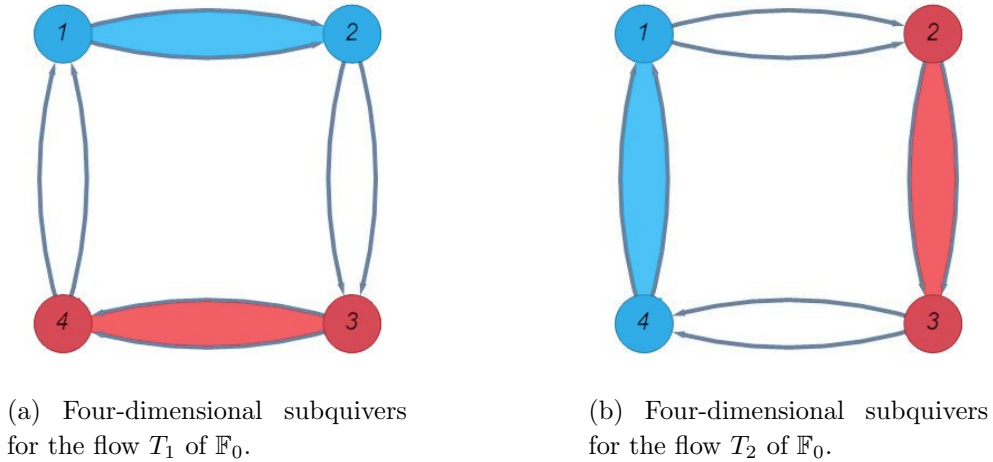


**Figure 10**

<sup>22</sup>We thank Sergey Mozgovoy and Boris Pioline for correspondence on this check.

**Remark 3.** Equation (4.32) translates into the following wall-crossing identity

$$\begin{aligned}
& \prod_{k \geq 0}^{\nearrow} \Phi(X_{\gamma_1+k(\gamma_1+\gamma_2)}) \Phi(X_{\gamma_3+k(\gamma_3+\gamma_4)}) \\
& \quad \times \prod_{s=\pm 1} \prod_{k \geq 0} \Phi((-y)^s X_{\gamma_1+\gamma_2+k\gamma_{D0}})^{-1} \cdot \Phi((-y)^s X_{\gamma_3+\gamma_4+k\gamma_{D0}})^{-1} \\
& \quad \times \prod_{k \geq 0}^{\searrow} \Phi(X_{\gamma_2+k(\gamma_1+\gamma_2)}) \Phi(X_{\gamma_4+k(\gamma_3+\gamma_4)}) \\
& = \prod_{k \geq 0}^{\nearrow} \Phi(X_{\gamma_2+k(\gamma_2+\gamma_3)}) \Phi(X_{\gamma_4+k(\gamma_4+\gamma_1)}) \\
& \quad \times \prod_{s=\pm 1} \prod_{k \geq 0} \Phi((-y)^s X_{\gamma_4+\gamma_1+k\gamma_{D0}})^{-1} \cdot \Phi((-y)^s X_{\gamma_2+\gamma_3+k\gamma_{D0}})^{-1} \\
& \quad \times \prod_{k \geq 0}^{\searrow} \Phi(X_{\gamma_3+k(\gamma_2+\gamma_3)}) \Phi(X_{\gamma_1+k(\gamma_4+\gamma_1)})
\end{aligned} \tag{4.44}$$

where we factored out the contribution of pure-flavor states (pure D0 branes), which do not participate in wall-crossing. We have tested this as an identity in the numerical ( $y \rightarrow -1$ ) setting, by acting on  $X_{\gamma_i}$  and expanding as formal series in  $X_\gamma$  with  $|\gamma| \leq 12$ .

#### 4.2 $dP_3$

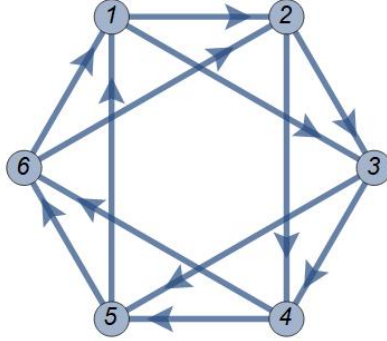


**Figure 11:** BPS quiver for local  $dP_3$

The BPS quiver for the theory corresponding to local  $dP_3$  is depicted in Figure 11, and has adjacency matrix

$$B = \begin{pmatrix} 0 & -1 & -1 & 0 & 1 & 1 \\ 1 & 0 & -1 & -1 & 0 & 1 \\ 1 & 1 & 0 & -1 & -1 & 0 \\ 0 & 1 & 1 & 0 & -1 & -1 \\ -1 & 0 & 1 & 1 & 0 & -1 \\ -1 & -1 & 0 & 1 & 1 & 0 \end{pmatrix} \tag{4.45}$$



The permutation symmetry of this quiver is  $\Pi_Q \simeq \mathbb{Z}_6$ . The adjacency matrix has rank 2, hence  $\text{rk} \Gamma_f = 4$ .

**Translations of the  $(A_1 + A_2)^{(1)}$  lattice.** The low-energy gauge theory phase of this theory is  $SU(2)$  Super Yang-Mills with two fundamental hypermultiplets, and the affine root lattice is  $\Gamma_f \simeq \mathcal{Q}((A_1 + A_2)^{(1)})$ . We can take as its generators the following vectors in  $\Gamma$ :

$$\alpha_0 = \gamma_3 + \gamma_6, \quad \alpha_1 = \gamma_1 + \gamma_4, \quad \alpha_2 = \gamma_2 + \gamma_5, \quad (4.46)$$

$$\beta_0 = \gamma_2 + \gamma_4 + \gamma_6, \quad \beta_1 = \gamma_1 + \gamma_3 + \gamma_5. \quad (4.47)$$

The null root is again  $\delta = \sum_i \gamma_i$ .

Note how the affine root lattice  $\mathcal{Q}((A_1 + A_2)^{(1)})$  has rank four, with generators the simple roots of  $A_2$ , the simple root of  $A_1$  and the null root  $\delta$  which is ‘shared’. This is in line with the statement that such an affine root lattice is isomorphic to  $\Gamma_f$  which also has rank four. As a matter of fact, this is reflected in the explicit form of the isomorphism (3.12) given above, where it is clear that the five generators obey the relation

$$\alpha_0 + \alpha_1 + \alpha_2 = \beta_0 + \beta_1 \equiv \delta. \quad (4.48)$$

In this case the Cremona group coincides with the extended Weyl group

$$\text{Cr}(dP_3) \simeq \widetilde{W}((A_1 + A_2)^{(1)}) = W((A_1 + A_2)^{(1)}) \rtimes \text{Dih}_6. \quad (4.49)$$

This is generated by the reflections on the  $A_2, A_1$  sublattices

$$s_0 = (3, 6)\mu_6\mu_3 \quad s_1 = (1, 4)\mu_4\mu_1, \quad s_2 = (2, 5)\mu_5\mu_2, \quad (4.50)$$

$$r_0 = (4, 6)\mu_2\mu_4\mu_6\mu_2, \quad r_1 = (3, 5)\mu_1\mu_3\mu_5\mu_1, \quad (4.51)$$

and by the outer automorphisms generating  $\text{Dih}_6$

$$\pi = (1, 2, 3, 4, 5, 6), \quad \sigma = (1, 4)(2, 3)(5, 6)\iota. \quad (4.52)$$

Of these,  $\pi$  is an order-six Dynkin diagram automorphism that permutes simple roots, see Figure 12. This is the generator of  $\Pi_Q \subset \text{Dih}_6$  that we’ll use to constrain  $\mathbb{U}$ .

We will focus here only on the  $A_2^{(1)}$  sublattice spanned by  $\alpha_1, \alpha_2, \alpha_3$ , since it is the only one whose roots contain only locally commuting charges, so that it gives rise to a collimation chamber as discussed in Section 3.4. (The sublattice  $A_1^{(1)}$  does not satisfy our technical assumption (a1), we leave its discussion to future work.) The subgroup of affine Weyl translations

$$\mathbb{Z}^3 \simeq \mathcal{T}(A_2^{(1)}) \subset \mathcal{T}((A_1 + A_2)^{(1)}) \quad (4.53)$$

is realized in  $\text{Aut}_Q$  by the following generators

$$T_1 = \pi^2 s_2 s_1, \quad T_2 = \pi^2 s_0 s_2, \quad T_3 = \pi^2 s_1 s_0. \quad (4.54)$$



**Figure 12:**  $(A_2 + A_1)^{(1)}$  Dynkin diagrams and automorphisms.  $\pi^2 = id$  on the  $A_1^{(1)}$  sublattice, while  $\pi^3 = id$  on the  $A_2^{(1)}$  sublattice. The two combine to give the  $\mathbb{Z}_6$  permutation symmetry of the quiver.

Its action on the sublattice of the affine root lattice  $\Gamma_f$  corresponding to  $\mathcal{Q}(A_2^{(1)})$  is

$$T_1^n(\vec{\alpha}) = \begin{pmatrix} \alpha_0 - n\delta, \\ \alpha_1 + n\delta, \\ \alpha_2 \end{pmatrix}, \quad T_2^n(\vec{\alpha}) = \begin{pmatrix} \alpha_0, \\ \alpha_1 - n\delta, \\ \alpha_2 + n\delta \end{pmatrix}, \quad T_3^n(\vec{\alpha}) = \begin{pmatrix} \alpha_0 + n\delta, \\ \alpha_1, \\ \alpha_2 - n\delta \end{pmatrix}. \quad (4.55)$$

This action extends to  $\Gamma$  as follows

$$T_1^n(\vec{\gamma}) = \begin{pmatrix} \gamma_1 + n(\gamma_1 + \gamma_2 + \gamma_3), \\ \gamma_2, \\ \gamma_3 - n(\gamma_1 + \gamma_2 + \gamma_3), \\ \gamma_4 + n(\gamma_4 + \gamma_5 + \gamma_6), \\ \gamma_5, \\ \gamma_6 - n(\gamma_4 + \gamma_5 + \gamma_6) \end{pmatrix}, \quad T_2^n(\vec{\gamma}) = \begin{pmatrix} \gamma_1 - n(\gamma_1 + \gamma_5 + \gamma_6), \\ \gamma_2 + n(\gamma_2 + \gamma_3 + \gamma_4), \\ \gamma_3, \\ \gamma_4 - n(\gamma_2 + \gamma_3 + \gamma_4), \\ \gamma_5 + n(\gamma_1 + \gamma_5 + \gamma_6), \\ \gamma_6. \end{pmatrix}, \quad (4.56)$$

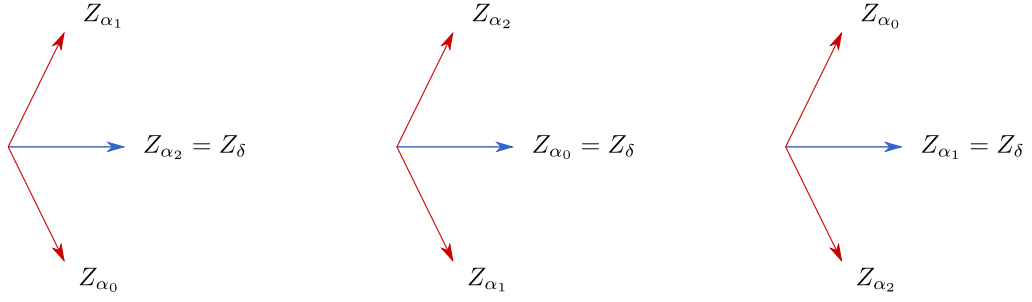
$$T_3^n(\vec{\gamma}) = \begin{pmatrix} \gamma_1, \\ \gamma_2 - n(\gamma_1 + \gamma_2 + \gamma_6), \\ \gamma_3 + n(\gamma_3 + \gamma_4 + \gamma_5), \\ \gamma_4, \\ \gamma_5 - n(\gamma_3 + \gamma_4 + \gamma_5), \\ \gamma_6 + n(\gamma_1 + \gamma_2 + \gamma_6). \end{pmatrix}.$$

As in the case of local  $\mathbb{F}_0$ , we observe that the three flows are related by the action of  $\mathbb{Z}_3 \subset \text{Out}(A_2^{(1)})$  permuting the three simple roots  $\alpha_i$ .<sup>23</sup>

$$T_1 = \pi^{-2}T_2\pi^2 = \pi^{-4}T_3\pi^4. \quad (4.57)$$

**Collimation chambers.** Having identified the relevant flows (4.54), we now study the associated stability conditions following the procedure outlined in Section 3.4. Recall that

<sup>23</sup>Note that  $\pi$  is a  $\mathbb{Z}_6 \simeq \Pi_Q$  generator on the full charge lattice  $\Gamma$ , and also on the affine root lattice  $\mathcal{Q}((A_1 + A_2)^{(1)})$ . This  $\mathbb{Z}_6$  is contained in the outer automorphism group  $\text{Out}((A_1 + A_2)^{(1)}) \simeq \text{Dih}_6$ . Then  $\pi^2$  generates a  $\mathbb{Z}_3$  outer automorphisms from  $\text{Out}(A_2^{(1)}) \simeq \text{Dih}_3$ , which acts trivially on  $\mathcal{Q}(A_1^{(1)})$ .



(a) Stability condition for  $T_1$     (b) Stability condition for  $T_2$     (c) Stability condition for  $T_3$

**Figure 13:** Stability conditions for  $dP_3$ .

$\delta = \sum_{i=1}^6 \gamma_i$ , while  $\alpha_i$  are expressed in terms of  $\gamma_i$  as in (4.46). Then the conditions corresponding to equations (3.21) and (3.23) translate here into

$$\begin{cases} \varphi_1 + \varphi_2 + \varphi_3 + \varphi_4 + \varphi_5 + \varphi_6 = 0 \\ \varphi_3 = \varphi_6, \\ \varphi_1 = \varphi_4, \\ \varphi_2 = \varphi_5. \end{cases} \quad (4.58)$$

This system by itself does not yet determine the stability condition. Recall indeed that we impose an additional requirement (3.22), corresponding to demanding that limiting rays lie on the real axis. The accumulation rays for the flow  $T_1$  in (3.18) can be read off from (4.56)

$$\delta_1(T_1) = \gamma_1 + \gamma_2 + \gamma_3, \quad \delta_2(T_1) = \gamma_4 + \gamma_5 + \gamma_6, \quad (4.59)$$

therefore we demand

$$\varphi_1 + \varphi_2 + \varphi_3 = \varphi_4 + \varphi_5 + \varphi_6 = 0. \quad (4.60)$$

As  $\gamma_2, \gamma_5$  are invariant under  $T_1$ , we can think of them in a certain sense as limiting vectors as well. It is then quite natural to also impose

$$\varphi_2 = \varphi_5 = 0. \quad (4.61)$$

Finally, observing that the first charge mutated by  $T_1$  in (4.54) is  $\gamma_1$ , the stability condition corresponding to the first flow is

$$\text{Stability condition for } T_1 : \quad \varphi_1 = \varphi_4 > \varphi_2 = \varphi_5 = 0 > \varphi_3 = \varphi_6 = -\varphi_1, \quad (4.62)$$

as in Figure 13a.

**Remark 4.** *The condition  $\theta_2 = \theta_5 = 0$  is not strictly necessary, but we need it to fix everything since  $A_2^{(1)}$  is only a sublattice of the full root system. It is suggested by the fact that these states are left invariant by the flow  $T_1$  (and so they are strictly speaking limiting vectors for the flow, although they are hypermultiplets). It is consistent since*

$$\begin{aligned} \langle \gamma_2, \gamma_5 \rangle &= \langle \gamma_2, \gamma_1 + \gamma_2 + \gamma_3 \rangle = \langle \gamma_5, \gamma_1 + \gamma_2 + \gamma_3 \rangle \\ &= \langle \gamma_2, \gamma_4 + \gamma_5 + \gamma_6 \rangle = \langle \gamma_5, \gamma_4 + \gamma_5 + \gamma_6 \rangle = 0. \end{aligned} \quad (4.63)$$

The conditions for the flows  $T_2$  and  $T_3$  respectively are obtained by applying  $\pi^2$  and  $\pi^4$  to the charges, so we have the other two stability conditions

$$\text{Stability condition for } T_2 : \quad \varphi_3 = \varphi_6 > \varphi_4 = \varphi_1 = 0 > \varphi_2 = \varphi_5 = -\varphi_3, \quad (4.64)$$

$$\text{Stability condition for } T_3 : \quad \varphi_2 = \varphi_5 > \varphi_3 = \varphi_6 = 0 > \varphi_1 = \varphi_4 = -\varphi_2, \quad (4.65)$$

illustrated in Figure 13b and 13c respectively.

So far we applied the criteria of Section 3.4 to deduce the stability conditions associated to flows  $T_i$ . As a check, we observe that iterations of the translation generators indeed admit a realization that only involves left-mutations. Note that

$$T_i^2 = \mathbf{m}_i^3, \quad (4.66)$$

where

$$\mathbf{m}_1 = \mu_6\mu_3\mu_5\mu_2\mu_4\mu_1, \quad \mathbf{m}_2 = \pi^2\mathbf{m}_1\pi^{-2}, \quad \mathbf{m}_3 = \pi^4\mathbf{m}_1\pi^{-4}, \quad (4.67)$$

Moreover we claim that iterations of these mutations correspond to tiltings of the positive half-plane for choices of stability data as given in (4.62), (4.64) and (4.64). Once again, the time flows are permuted version of charge tiltings, and contain the full information about the stability condition.

**BPS spectrum and Wall-crossing invariant.** A configuration of central charges satisfying conditions (4.62) corresponding to  $T_1$  can be taken as follows

$$\mathcal{C}_1[dP_3] \supset \begin{aligned} & Z_{\gamma_1} = Z_{\gamma_4}, \quad Z_{\gamma_2} = Z_{\gamma_5}, \quad Z_{\gamma_3} = Z_{\gamma_6}, \\ & \arg Z_{\gamma_1} > \arg Z_{\gamma_2} > \arg Z_{\gamma_3}, \quad Z_{\gamma_1} + Z_{\gamma_3} = Z_{\gamma_2} \in \mathbb{R}^+. \end{aligned} \quad (4.68)$$

Similarly we denote by  $\mathcal{C}_i[dP_3]$  the chambers corresponding to flows  $T_i$  with  $i = 2, 3$ . Since the limiting rays of  $T_1$  are (4.59), and since we demanded that their central charges are real (4.60), the flow is expected to produce towers of states asymptotic to the real axis (also see [34] for a discussion). This matches the definition of collimation chamber.

Having identified the choice of stability condition corresponding to a (putative) collimation chamber, we may deduce parts of the spectrum contained in the sectors  $\mathcal{L}^\pm$  of the  $Z$ -plane (corresponding to  $\text{Re}Z > 0$  and  $\text{Im}Z > 0$  or  $< 0$ ) by tilting the positive half-plane and following the induced sequences of left- and right-mutations. The mutation sequences are, respectively <sup>24</sup>

$$\begin{aligned} \text{CW tilt} \quad \mathbf{m}_1 &= \mu_6\mu_3\mu_5\mu_2\mu_4\mu_1 \\ \text{CCW tilt} \quad \tilde{\mathbf{m}}_1 &= \tilde{\mu}_4\tilde{\mu}_1\tilde{\mu}_5\tilde{\mu}_2\tilde{\mu}_6\tilde{\mu}_3 \end{aligned} \quad (4.69)$$

---

<sup>24</sup>These coincide with the mutation sequences observed in [34, eq. (2.36)]. To see it, it suffices to separate all permutations (taking them to the left) from all mutations (taken to the right) in their formulae.

Acting on  $Q$  with  $\mathbf{m}_1^n$  and  $\tilde{\mathbf{m}}_1^n$  yields respectively the following towers of hypermultiplets

$$\begin{aligned}
\Omega(\gamma_1 + n(\gamma_1 + \gamma_2 + \gamma_3)) &= 1 \\
\Omega(\gamma_3 + n(\gamma_1 + \gamma_2 + \gamma_3)) &= 1 \\
\Omega(-\gamma_1 + (n+1)(\gamma_1 + \gamma_2 + \gamma_3)) &= 1 \\
\Omega(-\gamma_3 + (n+1)(\gamma_1 + \gamma_2 + \gamma_3)) &= 1
\end{aligned} \tag{4.70}$$

for  $n \geq 0$ , and similarly with  $\{1, 2, 3\} \rightarrow \{4, 5, 6\}$ . As promised, their central charges accumulate towards  $\mathbb{R}^+$  from both sides for  $n \rightarrow +\infty$ . It is then straightforward to write down  $\mathbb{U}(\mathcal{L}^\pm)$  explicitly as a product of phase-ordered quantum dilogarithms.

$$\begin{aligned}
\mathbb{U}(\mathcal{L}^+, \mathcal{C}_1) &= \prod_{k \geq 0}^{\nearrow} \left( \Phi(X_{\gamma_1+k(\gamma_1+\gamma_2+\gamma_3)}) \Phi(X_{\gamma_4+k(\gamma_4+\gamma_5+\gamma_6)}) \right. \\
&\quad \left. \times \Phi(X_{\gamma_1+\gamma_2+k(\gamma_1+\gamma_2+\gamma_3)}) \Phi(X_{\gamma_4+\gamma_5+k(\gamma_4+\gamma_5+\gamma_6)}) \right) \\
\mathbb{U}(\mathcal{L}^-, \mathcal{C}_1) &= \prod_{k \geq 0}^{\searrow} \left( \Phi(X_{\gamma_5+\gamma_6+k(\gamma_4+\gamma_5+\gamma_6)}) \Phi(X_{\gamma_2+\gamma_3+k(\gamma_1+\gamma_2+\gamma_3)}) \right. \\
&\quad \left. \times \Phi(X_{\gamma_6+k(\gamma_4+\gamma_5+\gamma_6)}) \Phi(X_{\gamma_3+k(\gamma_1+\gamma_2+\gamma_3)}) \right)
\end{aligned} \tag{4.71}$$

To determine  $\mathbb{U}(\mathbb{R}^+)$  we adopt a formal series expansion as in (2.16) and express  $\mathbb{U}$  as a function of the coefficients  $c_\gamma$  of  $\mathbb{U}(\mathbb{R}^+)$  through (2.11). We then impose (2.15) using the  $\Pi_Q \simeq \mathbb{Z}_6$  symmetry of the quiver of Figure 11

$$\pi : \gamma_i \mapsto \gamma_{i+1 \bmod 6}. \tag{4.72}$$

Solving for the coefficients  $c_\gamma$  we obtain a series in  $X_\gamma$  up to arbitrary order  $|\gamma|$ , which is compatible with the following factorization

$$\begin{aligned}
\mathbb{U}_0(\mathbb{R}^+, \mathcal{C}_1) &= \prod_{k \geq 0} \left( \Phi(X_{\gamma_2+k\gamma_{D0}}) \cdot \Phi(X_{\gamma_1+\gamma_3+k\gamma_{D0}}) \right. \\
&\quad \cdot \Phi(X_{-\gamma_2+(k+1)\gamma_{D0}}) \cdot \Phi(X_{-\gamma_1-\gamma_3+(k+1)\gamma_{D0}}) \\
&\quad \cdot \prod_{s=\pm 1} \Phi((-y)^s X_{\gamma_1+\gamma_2+\gamma_3+k\gamma_{D0}})^{-1} \left. \right) \\
&\quad \times (\{1, 2, 3\} \rightarrow \{4, 5, 6\})
\end{aligned} \tag{4.73}$$

where  $\gamma_{D0} = \sum_i \gamma_i$ . This corresponds to a spectrum along the real ray consisting of

$$\begin{aligned}
\Omega(\gamma_2 + n\gamma_{D0}) &= \Omega(-\gamma_2 + (n+1)\gamma_{D0}) = 1 \\
\Omega(\gamma_5 + n\gamma_{D0}) &= \Omega(-\gamma_5 + (n+1)\gamma_{D0}) = 1 \\
\Omega(\gamma_1 + \gamma_3 + n\gamma_{D0}) &= \Omega(-\gamma_1 - \gamma_3 + (n+1)\gamma_{D0}) = 1 \\
\Omega(\gamma_4 + \gamma_6 + n\gamma_{D0}) &= \Omega(-\gamma_4 - \gamma_6 + (n+1)\gamma_{D0}) = 1 \\
\Omega(\gamma_1 + \gamma_2 + \gamma_3 + n\gamma_{D0}) &= \Omega(-\gamma_1 - \gamma_2 - \gamma_3 + (n+1)\gamma_{D0}) = y + y^{-1}
\end{aligned} \tag{4.74}$$

As in the case of local  $\mathbb{F}_0$ , the spectrum of BPS states on the real ray features towers of BPS states corresponding to Kaluza-Klein towers of charges  $\gamma_2, \gamma_5, \gamma_1 + \gamma_3, \gamma_4 + \gamma_6$ , and their CPT conjugate KK towers. From the viewpoint of the splitting into two 4d  $SU(2)$   $N_f = 1$  subquivers, these KK towers correspond to bound states of  $N_f = 1$  quarks with D0 branes.

Once again this misses the contributions from pure D0 branes. We refer to the remarks below (4.40) for a discussion. In this case the expected motivic DT invariant for any number of D0 branes is [22]

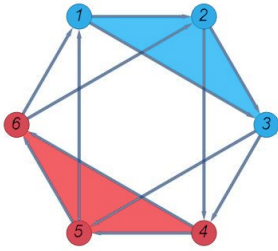
$$\Omega(n\gamma_{D0}; y) = y^3 + 4y + y^{-1}. \quad (4.75)$$

The corresponding contribution to  $\mathbb{U}(\mathbb{R}^+)$  is a product of quantum dilogarithms as outlined in (2.10) *et seq.*

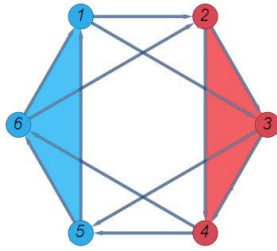
$$\mathbb{U}(\mathbb{R}^+, \mathcal{C}_1) = \mathbb{U}_0(\mathbb{R}^+, \mathcal{C}_1) \cdot \prod_{n \geq 1} \Phi((-y)^{-1} X_{n\gamma_{D0}})^{-1} \Phi((-y) X_{n\gamma_{D0}})^{-4} \Phi((-y)^3 X_{n\gamma_{D0}})^{-1}. \quad (4.76)$$

In conclusion, the spectrum we obtain for local  $dP_3$  in chamber  $\mathcal{C}_1$  is

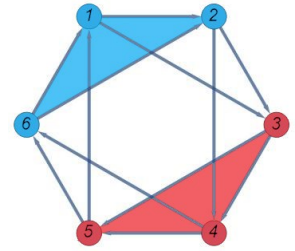
$\gamma$	$\Omega(\gamma; y)$	
$\gamma_r + k(\gamma_1 + \gamma_2 + \gamma_3)$	1	
$-\gamma_r + (k+1)(\gamma_1 + \gamma_2 + \gamma_3)$	1	
$\gamma_s + k(\gamma_4 + \gamma_5 + \gamma_6)$	1	
$-\gamma_s + (k+1)(\gamma_4 + \gamma_5 + \gamma_6)$	1	
$\gamma_t + k\gamma_{D0}$	1	(4.77)
$-\gamma_t + (k+1)\gamma_{D0}$	1	
$\gamma_a + \gamma_b + k\gamma_{D0}$	1	
$-\gamma_a - \gamma_b + (k+1)\gamma_{D0}$	1	
$\gamma_1 + \gamma_2 + \gamma_3 + k\gamma_{D0}$	$y + y^{-1}$	
$-\gamma_1 - \gamma_2 - \gamma_3 + (k+1)\gamma_{D0}$	$y + y^{-1}$	
$(k+1)\gamma_{D0}$	$y^3 + 4y + y^{-1}$	



(a) Four-dimensional subquivers for the flow  $T_1$  of  $dP_3$ .



(b) Four-dimensional subquivers for the flow  $T_2$  of  $dP_3$ .



(c) Four-dimensional subquivers for the flow  $T_3$  of  $dP_3$ .

**Figure 14**

with  $k \geq 0$  and

$$r \in \{1, 3\} \quad s \in \{4, 6\} \quad t \in \{2, 5\} \quad (a, b) \in \{(1, 3), (4, 6)\}. \quad (4.78)$$

The spectrum also includes the respective antiparticles obtained by sending  $\gamma \rightarrow -\gamma$ .

**Remark 5.** *The wall-crossing constraint that we solved is the following identity*

$$\begin{aligned}
& \prod_{k \geq 0}^{\nearrow} \left( \Phi(X_{\gamma_1+k(\gamma_1+\gamma_2+\gamma_3)}) \Phi(X_{\gamma_4+k(\gamma_4+\gamma_5+\gamma_6)}) \right. \\
& \quad \left. \times \Phi(X_{-\gamma_3+(k+1)(\gamma_1+\gamma_2+\gamma_3)}) \Phi(X_{-\gamma_6+(k+1)(\gamma_4+\gamma_5+\gamma_6)}) \right) \\
& \times \prod_{k \geq 0} \left( \Phi(X_{\gamma_2+k\gamma_{D0}}) \Phi(X_{-\gamma_2+(k+1)\gamma_{D0}}) \Phi(X_{\gamma_1+\gamma_3+k\gamma_{D0}}) \Phi(X_{-\gamma_1-\gamma_3+(k+1)\gamma_{D0}}) \right. \\
& \quad \times \Phi(X_{\gamma_5+k\gamma_{D0}}) \Phi(X_{-\gamma_5+(k+1)\gamma_{D0}}) \Phi(X_{\gamma_4+\gamma_6+k\gamma_{D0}}) \Phi(X_{-\gamma_4-\gamma_6+(k+1)\gamma_{D0}}) \\
& \quad \left. \times \left( \prod_{s=\pm 1} \Phi((-y)^s X_{\gamma_1+\gamma_2+\gamma_3+k\gamma_{D0}})^{-1} \Phi((-y)^s X_{-\gamma_1-\gamma_2-\gamma_3+(k+1)\gamma_{D0}})^{-1} \right) \right) \quad (4.79) \\
& \times \prod_{k \geq 0}^{\searrow} \left( \Phi(X_{-\gamma_4+(k+1)(\gamma_4+\gamma_5+\gamma_6)}) \Phi(X_{-\gamma_1+(k+1)(\gamma_1+\gamma_2+\gamma_3)}) \right. \\
& \quad \left. \times \Phi(X_{\gamma_6+k(\gamma_4+\gamma_5+\gamma_6)}) \Phi(X_{\gamma_3+k(\gamma_1+\gamma_2+\gamma_3)}) \right) \\
& = (\{\gamma_1, \gamma_2, \gamma_3, \gamma_4, \gamma_5, \gamma_6\} \rightarrow \{\gamma_2, \gamma_3, \gamma_4, \gamma_5, \gamma_6, \gamma_1\})
\end{aligned}$$

where we factored out the contribution of pure-flavor states (pure D0 branes), which do not participate in wall-crossing. We have tested this as an identity in the numerical ( $y \rightarrow -1$ ) setting, by acting on  $X_{\gamma_i}$  and expanding as formal series in  $X_{\gamma}$  with  $|\gamma| \leq 12$ .

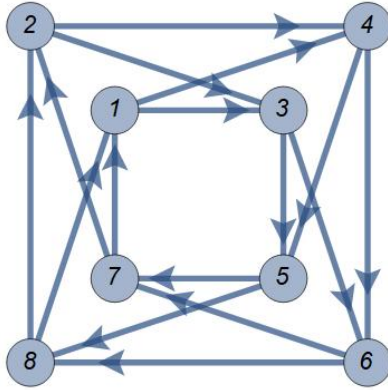


Figure 15: BPS quiver for  $dP_5$

### 4.3 $dP_5$

The BPS quiver for the theory corresponding to local  $dP_5$  is depicted in Figure 15, and has adjacency matrix<sup>25</sup>

$$B = \begin{pmatrix} 0 & 0 & -1 & -1 & 0 & 0 & 1 & 1 \\ 0 & 0 & -1 & -1 & 0 & 0 & 1 & 1 \\ 1 & 1 & 0 & 0 & -1 & -1 & 0 & 0 \\ 1 & 1 & 0 & 0 & -1 & -1 & 0 & 0 \\ 0 & 0 & 1 & 1 & 0 & 0 & -1 & -1 \\ 0 & 0 & 1 & 1 & 0 & 0 & -1 & -1 \\ -1 & -1 & 0 & 0 & 1 & 1 & 0 & 0 \\ -1 & -1 & 0 & 0 & 1 & 1 & 0 & 0 \end{pmatrix} \quad (4.80)$$

The permutation symmetry of this quiver is  $\Pi_Q \simeq (\mathbb{Z}_2)^{\times 4} \rtimes \mathbb{Z}_4$ . The adjacency matrix of this quiver has rank two, so  $\text{rk } \Gamma_f = 6$ .

**Translations of the  $D_5^{(1)}$  lattice.** The low-energy gauge theory phase of this theory is  $SU(2)$  Super Yang-Mills with four fundamental hypermultiplets, and the affine root lattice is  $\mathcal{Q}(D_5^{(1)}) \simeq \Gamma_f$ . We can take as its generators the following vectors in  $\Gamma$ :

$$\alpha_0 = \gamma_2 - \gamma_1, \quad \alpha_1 = \gamma_6 - \gamma_5, \quad \alpha_2 = \gamma_1 + \gamma_5, \quad (4.81)$$

$$\alpha_3 = \gamma_3 + \gamma_7, \quad \alpha_4 = \gamma_4 - \gamma_3, \quad \alpha_5 = \gamma_8 - \gamma_7. \quad (4.82)$$

The null root is again  $\delta = \sum_i \gamma_i$ .

<sup>25</sup>This quiver is related by mutations to the one obtained in [62, Figure 19]. It also matches with the quiver in [70, Figure 8A]. As pointed out in [70] this is also equivalent to the quiver in Figure 7 of the same paper, which further coincides with the recent derivation in [27, eq. (8.44)]. Although local  $dP_5$  is not toric, this quiver can also be obtained by techniques for toric CY threefolds, see model 4a in [71], which corresponds to a *pseudo* del Pezzo surface  $PdP_5$ . The distinction between quivers of  $dP_5$  and  $PdP_5$  lies in the possible presence of bidirectional arrows for the latter [21], however this depends on the superpotential, which plays no role in our construction.



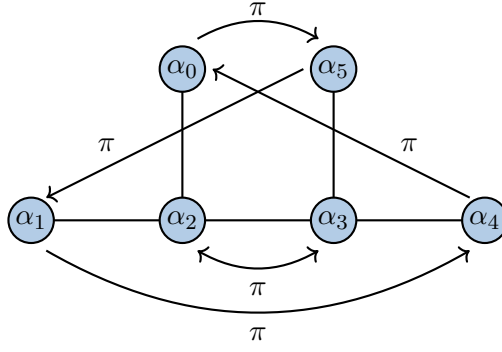


**Figure 16:**  $D_5^{(1)}$  Dynkin diagram and automorphisms

The Cremona group coincides with the extended affine Weyl group

$$\mathrm{Cr}(dP_5) = \widetilde{W}(D_5^{(1)}) = W(D_5^{(1)}) \rtimes \mathrm{Out}(D_5^{(1)}). \quad (4.83)$$

Note that  $\mathrm{Out}(D_5^{(1)})$  contains the permutation symmetries  $\Pi_Q$  as a subgroup. Indeed,  $\mathrm{Cr}(dP_5)$  can be realized in  $\mathrm{Aut}_Q$  as follows

$$s_0 = (1, 2), \quad s_1 = (5, 6), \quad s_2 = (1, 5)\mu_1\mu_5, \quad (4.84)$$

$$s_3 = (3, 7)\mu_3\mu_7, \quad s_4 = (3, 4), \quad s_5 = (7, 8), \quad (4.85)$$

$$\pi = (1, 3, 5, 7)(2, 4, 6, 8), \quad \sigma = (1, 7)(2, 8)(3, 5)(4, 6)\iota, \quad (4.86)$$

where  $s_i$  is an elementary reflection along the root  $\alpha_i$ , and

$$\pi(\vec{\alpha}) = \begin{pmatrix} \alpha_4 \\ \alpha_5 \\ \alpha_3 \\ \alpha_2 \\ \alpha_1 \\ \alpha_0 \end{pmatrix} \quad (4.87)$$

is the Dynkin diagram automorphism of Figure 16. All affine simple roots  $\alpha_i$  correspond to sums of mutually local charges, in fulfillment of assumption (a3) in Section 3.4.

Instead of discussing the whole subgroup of affine Weyl translations  $\mathcal{T}(D_5^{(1)})$ , we just focus on the  $\mathbb{Z}$ -subgroup generated by

$$T_1^n(\vec{\alpha}) = \begin{pmatrix} \alpha_0 \\ \alpha_1 \\ \alpha_2 + n\delta \\ \alpha_3 - n\delta \\ \alpha_4 \\ \alpha_5 \end{pmatrix}. \quad (4.88)$$

This admits the following realization in  $\text{Aut}_Q$

$$T_1 = s_3 s_4 s_5 s_3 s_2 s_1 s_0 s_2 (2, 6)(1, 5)(4, 8)(7, 3), \quad (4.89)$$

which extends the definition of  $T_1$  to the whole charge lattice  $\Gamma$

$$T_1^n(\vec{\gamma}) = \begin{pmatrix} \gamma_1 + n(\gamma_1 + \gamma_2 + \gamma_3 + \gamma_4) \\ \gamma_2 + n(\gamma_1 + \gamma_2 + \gamma_3 + \gamma_4) \\ \gamma_3 - n(\gamma_1 + \gamma_2 + \gamma_3 + \gamma_4) \\ \gamma_4 - n(\gamma_1 + \gamma_2 + \gamma_3 + \gamma_4) \\ \gamma_5 + n(\gamma_5 + \gamma_6 + \gamma_7 + \gamma_8) \\ \gamma_6 + n(\gamma_5 + \gamma_6 + \gamma_7 + \gamma_8) \\ \gamma_7 - n(\gamma_5 + \gamma_6 + \gamma_7 + \gamma_8) \\ \gamma_8 - n(\gamma_5 + \gamma_6 + \gamma_7 + \gamma_8) \end{pmatrix}. \quad (4.90)$$

We can obtain another, independent flow, by applying the Dynkin diagram automorphism

$$T_2 = \pi T_1 \pi^{-1} \quad (4.91)$$

acting on roots, and on the whole  $\Gamma$ , respectively as follows

$$T_2^n(\vec{\alpha}) = \begin{pmatrix} \alpha_0 \\ \alpha_1 \\ \alpha_2 - n\delta \\ \alpha_3 + n\delta \\ \alpha_4 \\ \alpha_5 \end{pmatrix}, \quad T_2^n(\vec{\gamma}) = \begin{pmatrix} \gamma_1 - n(\gamma_1 + \gamma_2 + \gamma_7 + \gamma_8) \\ \gamma_2 - n(\gamma_1 + \gamma_2 + \gamma_7 + \gamma_8) \\ \gamma_3 + n(\gamma_3 + \gamma_4 + \gamma_5 + \gamma_6) \\ \gamma_4 + n(\gamma_3 + \gamma_4 + \gamma_5 + \gamma_6) \\ \gamma_5 - n(\gamma_3 + \gamma_4 + \gamma_5 + \gamma_6) \\ \gamma_6 - n(\gamma_3 + \gamma_4 + \gamma_5 + \gamma_6) \\ \gamma_7 + n(\gamma_1 + \gamma_2 + \gamma_7 + \gamma_8) \\ \gamma_8 + n(\gamma_1 + \gamma_2 + \gamma_7 + \gamma_8) \end{pmatrix}. \quad (4.92)$$

**Remark 6.** *Note that the Weyl translation naturally splits the BPS quiver into two four-dimensional subquivers [34]. The towers of states that we find are those appearing in the weakly-coupled spectrum of these subquivers, shown in Figure 1*

**Collimation chambers.** We now turn to the discussion of collimation chambers associated to the flows  $T_1$  and  $T_2$ . Recalling that  $\delta = \sum_{i=1}^8 \gamma_i$ , while  $\alpha_i$  are expressed in terms of  $\gamma_i$  as in (4.81), conditions corresponding to equations (3.21) and (3.23) translate here

into<sup>26</sup>

$$\left\{ \begin{array}{l} \sum_i \varphi_i = 0, \\ \varphi_2 = \varphi_1, \\ \varphi_6 = \varphi_5, \\ \varphi_1 = \varphi_5, \\ \varphi_3 = \varphi_7, \\ \varphi_4 = \varphi_3, \\ \varphi_8 = \varphi_7. \end{array} \right. \quad (4.93)$$

which is solved by

$$\varphi_1 = \varphi_2 = \varphi_5 = \varphi_6 = -\varphi_3 = -\varphi_4 = -\varphi_7 = -\varphi_8. \quad (4.94)$$

These constraints leave room for precisely two configurations of central charges within the positive half-plane, namely

$$\mathcal{C}_1[dP_5] : \quad \varphi_1 > \varphi_3, \quad \mathcal{C}_2[dP_5] : \quad \varphi_1 < \varphi_3. \quad (4.95)$$

The corresponding ray diagrams are shown in Figure 17.

So far we applied the criteria of Section 3.4 to deduce the stability conditions associated to flows  $T_1$  and  $T_2$ . As a check, we observe that iterations of these translation generators indeed admit a realization that only involves left-mutations

$$\begin{aligned} T_1 = \mathbf{m}_1 &:= \mu_3 \mu_4 \mu_7 \mu_8 \mu_1 \mu_2 \mu_5 \mu_6, \\ T_2 = \mathbf{m}_2 &:= \mu_1 \mu_2 \mu_5 \mu_6 \mu_3 \mu_4 \mu_7 \mu_8. \end{aligned} \quad (4.96)$$

Moreover we claim that iterations of these mutations correspond to tiltings of the positive half-plane for choices of stability data as given in (4.95).

**BPS spectrum and Wall-crossing invariant.** A configuration of central charges satisfying conditions (4.94)-(4.95) corresponding to  $T_1$  can be taken as follows

$$\mathcal{C}_1[dP_5] \supset \begin{array}{l} Z_{\gamma_2} = Z_{\gamma_6} = c \cdot Z_{\gamma_1} = c \cdot Z_{\gamma_5}, \quad Z_{\gamma_4} = Z_{\gamma_8} = c \cdot Z_{\gamma_3} = c \cdot Z_{\gamma_7}, \\ Z_{\gamma_1} = \bar{Z}_{\gamma_3}, \quad \arg Z_{\gamma_1} > \arg Z_{\gamma_3}, \end{array} \quad (4.97)$$

with an arbitrary real constant  $c > 1$ , needed to ensure that  $Z_{\alpha_i}$  belong to the positive half-plane. Likewise, a configuration of central charges in chamber  $\mathcal{C}_2[dP_5]$  is related to  $\mathcal{C}_1[dP_5]$  by switching the last condition with  $\arg Z_{\gamma_1} < \arg Z_{\gamma_3}$ .

Focusing on  $\mathcal{C}_1[dP_5]$ , and tilting the positive half-plane of central charges clockwise, induces infinite iterations of the sequence of mutations  $\mathbf{m}_1$ . Likewise, tilting CCW we find an infinite repetition of the following sequence

$$\tilde{\mathbf{m}}_1 := \tilde{\mu}_6 \tilde{\mu}_5 \tilde{\mu}_2 \tilde{\mu}_1 \tilde{\mu}_8 \tilde{\mu}_7 \tilde{\mu}_4 \tilde{\mu}_3. \quad (4.98)$$

---

<sup>26</sup>This explains why we considered just the flow  $T_1$  instead of the whole translation group  $\mathcal{T}(D_5^{(1)})$ . In principle the root lattice  $\mathcal{Q}(D_5^{(1)})$  allows for many different flows. However, the technical condition (3.23), that requires all charges entering in a root in (4.81) to lie on the same ray, greatly restricts our allowed choices of tiltings. It is plausible that by relaxing this condition one could make sense also of the other affine translations.

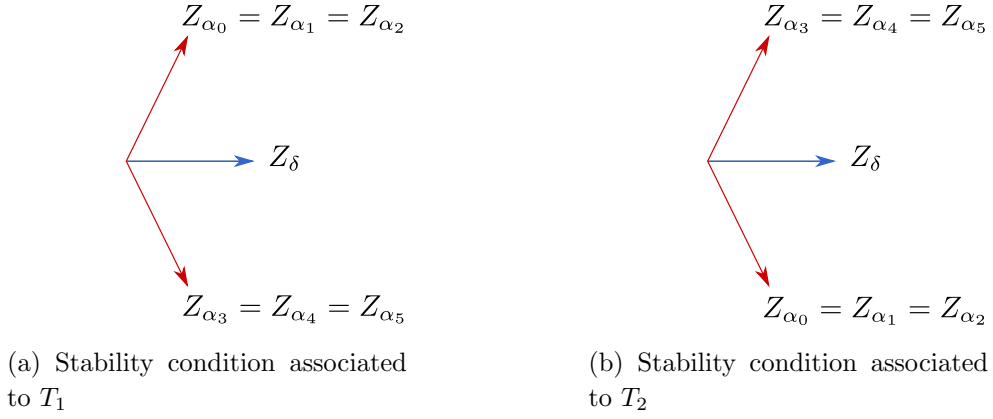


**Figure 17:** Stability conditions for  $dP_5$ , corresponding to  $\mathcal{C}_1[dP_5]$  and  $\mathcal{C}_2[dP_5]$ .

Together the mutation sequences  $\mathbf{m}_1, \tilde{\mathbf{m}}_1$  generate towers of hypermultiplets

$$\begin{aligned}
\Omega(\gamma_1 + n(\gamma_1 + \gamma_2 + \gamma_3 + \gamma_4)) &= 1 & \Omega(\gamma_5 + n(\gamma_5 + \gamma_6 + \gamma_7 + \gamma_8)) &= 1 \\
\Omega(\gamma_2 + n(\gamma_1 + \gamma_2 + \gamma_3 + \gamma_4)) &= 1 & \Omega(\gamma_6 + n(\gamma_5 + \gamma_6 + \gamma_7 + \gamma_8)) &= 1 \\
\Omega(\gamma_3 + n(\gamma_1 + \gamma_2 + \gamma_3 + \gamma_4)) &= 1 & \Omega(\gamma_7 + n(\gamma_5 + \gamma_6 + \gamma_7 + \gamma_8)) &= 1 \\
\Omega(\gamma_4 + n(\gamma_1 + \gamma_2 + \gamma_3 + \gamma_4)) &= 1 & \Omega(\gamma_8 + n(\gamma_5 + \gamma_6 + \gamma_7 + \gamma_8)) &= 1 \\
\Omega(\gamma_1 + \gamma_2 + \gamma_3 + n(\gamma_1 + \gamma_2 + \gamma_3 + \gamma_4)) &= 1 & \Omega(\gamma_5 + \gamma_6 + \gamma_7 + n(\gamma_5 + \gamma_6 + \gamma_7 + \gamma_8)) &= 1 \\
\Omega(\gamma_1 + \gamma_2 + \gamma_4 + n(\gamma_1 + \gamma_2 + \gamma_3 + \gamma_4)) &= 1 & \Omega(\gamma_5 + \gamma_6 + \gamma_8 + n(\gamma_5 + \gamma_6 + \gamma_7 + \gamma_8)) &= 1 \\
\Omega(\gamma_3 + \gamma_4 + \gamma_1 + n(\gamma_1 + \gamma_2 + \gamma_3 + \gamma_4)) &= 1 & \Omega(\gamma_7 + \gamma_8 + \gamma_5 + n(\gamma_5 + \gamma_6 + \gamma_7 + \gamma_8)) &= 1 \\
\Omega(\gamma_3 + \gamma_4 + \gamma_2 + n(\gamma_1 + \gamma_2 + \gamma_3 + \gamma_4)) &= 1 & \Omega(\gamma_7 + \gamma_8 + \gamma_6 + n(\gamma_5 + \gamma_6 + \gamma_7 + \gamma_8)) &= 1
\end{aligned} \tag{4.99}$$

Since  $Z_{\gamma_1+\dots+\gamma_4} = Z_{\gamma_5+\dots+\gamma_8} \in \mathbb{R}^+$  the BPS rays of these hypermultiplets asymptote to  $\mathbb{R}^+$  from both sides, confirming that (4.97) defines a collimation chamber. It should be noted that, although many central charges have the same phase, this does not correspond to a wall of marginal stability because all relevant charges are mutually local.

$$\begin{aligned}
\mathbb{U}(\mathcal{L}^+, \mathcal{C}_1) &= \prod_{k \geq 0}^{\nearrow} \left[ \left( \prod_{\ell=1,2} \Phi(X_{\gamma_\ell + k(\gamma_1 + \gamma_2 + \gamma_3 + \gamma_4)}) \right) \left( \prod_{\ell=5,6} \Phi(X_{\gamma_\ell + k(\gamma_5 + \gamma_6 + \gamma_7 + \gamma_8)}) \right) \right. \\
&\quad \times \left. \left( \prod_{\ell=3,4} \Phi(X_{\gamma_1 + \gamma_2 + \gamma_\ell + k(\gamma_1 + \gamma_2 + \gamma_3 + \gamma_4)}) \right) \left( \prod_{\ell=7,8} \Phi(X_{\gamma_5 + \gamma_6 + \gamma_\ell + k(\gamma_5 + \gamma_6 + \gamma_7 + \gamma_8)}) \right) \right] \\
\mathbb{U}(\mathcal{L}^-, \mathcal{C}_1) &= \prod_{k \geq 0}^{\searrow} \left[ \left( \prod_{\ell=1,2} \Phi(X_{\gamma_3 + \gamma_4 + \gamma_\ell + k(\gamma_1 + \gamma_2 + \gamma_3 + \gamma_4)}) \right) \left( \prod_{\ell=5,6} \Phi(X_{\gamma_7 + \gamma_8 + \gamma_\ell + k(\gamma_5 + \gamma_6 + \gamma_7 + \gamma_8)}) \right) \right. \\
&\quad \times \left. \left( \prod_{\ell=3,4} \Phi(X_{\gamma_\ell + k(\gamma_1 + \gamma_2 + \gamma_3 + \gamma_4)}) \right) \left( \prod_{\ell=7,8} \Phi(X_{\gamma_\ell + k(\gamma_5 + \gamma_6 + \gamma_7 + \gamma_8)}) \right) \right]
\end{aligned} \tag{4.100}$$

Following the familiar script already used for  $\mathbb{F}_0$  and  $dP_3$ , to determine  $\mathbb{U}(\mathbb{R}^+)$  we adopt a formal series expansion as in (2.16) and express  $\mathbb{U}$  as a function of the coefficients  $c_\gamma$  of  $\mathbb{U}(\mathbb{R}^+)$  through (2.11). We then impose (2.15) using the generator  $\pi$  of the  $\mathbb{Z}_4 \subset \Pi_Q$  symmetry<sup>27</sup> of the quiver of Figure 15 Solving for the coefficients  $c_\gamma$  we obtain a series in  $X_\gamma$  up to arbitrary order  $|\gamma|$ , which is compatible with the factorization

$$\mathbb{U}(\mathbb{R}^+) = \prod_{\gamma} \prod_{m \in \mathbb{Z}} \Phi((-y)^m X_\gamma)^{a_m(\gamma)} \tag{4.101}$$

where  $\Omega(\gamma, y) = \sum_m (-y)^m a_m(\gamma)$  are as follows

$$\begin{aligned}
\Omega(\gamma_1 + \gamma_3 + n\gamma_{D0}) &= \Omega(-\gamma_1 - \gamma_3 + (n+1)\gamma_{D0}) = 1 \\
\Omega(\gamma_1 + \gamma_4 + n\gamma_{D0}) &= \Omega(-\gamma_1 - \gamma_4 + (n+1)\gamma_{D0}) = 1 \\
\Omega(\gamma_2 + \gamma_3 + n\gamma_{D0}) &= \Omega(-\gamma_2 - \gamma_3 + (n+1)\gamma_{D0}) = 1 \\
\Omega(\gamma_2 + \gamma_4 + n\gamma_{D0}) &= \Omega(-\gamma_2 - \gamma_4 + (n+1)\gamma_{D0}) = 1 \\
\Omega(\gamma_5 + \gamma_7 + n\gamma_{D0}) &= \Omega(-\gamma_5 - \gamma_7 + (n+1)\gamma_{D0}) = 1 \\
\Omega(\gamma_5 + \gamma_8 + n\gamma_{D0}) &= \Omega(-\gamma_5 - \gamma_8 + (n+1)\gamma_{D0}) = 1 \\
\Omega(\gamma_6 + \gamma_7 + n\gamma_{D0}) &= \Omega(-\gamma_6 - \gamma_7 + (n+1)\gamma_{D0}) = 1 \\
\Omega(\gamma_6 + \gamma_8 + n\gamma_{D0}) &= \Omega(-\gamma_6 - \gamma_8 + (n+1)\gamma_{D0}) = 1
\end{aligned} \tag{4.102}$$

$$\Omega(\gamma_1 + \gamma_2 + \gamma_3 + \gamma_4 + n\gamma_{D0}) = \Omega(-\gamma_1 - \gamma_2 - \gamma_3 - \gamma_4 + (n+1)\gamma_{D0}) = y + y^{-1}$$

Once again this misses the contributions from pure D0 branes. We refer to the remarks below (4.40) for a discussion. Based on the observation that the moduli space of a D0 brane (or a boundstate of  $n$  D0 branes) is the Calabi-Yau itself, we expect that once again the Protected Spin Character of  $n$  D0 equals the Poincaré polynomial of the local del Pezzo [22]. Recalling from Section 3.1 that  $\dim H^2(S, \mathbb{Z}) = n + 1$  we conjecture

$$\Omega(n\gamma_{D0}; y) = y^3 + 6y + y^{-1}. \tag{4.103}$$

<sup>27</sup>Note that  $(\mathbb{Z}_2)^{\times 4}$  acts trivially on  $\mathcal{C}_1$ . Moreover, only a  $\mathbb{Z}_2$  subgroup of  $\mathbb{Z}_4$  acts nontrivially on  $\mathcal{C}_1$ , exchanging stability conditions in Figure 17.

In conclusion, the spectrum we obtain for local  $dP_5$  in chamber  $\mathcal{C}_1$  is

$\gamma$	$\Omega(\gamma; y)$
$\gamma_r + k(\gamma_1 + \gamma_2 + \gamma_3 + \gamma_4)$	1
$-\gamma_r + (k+1)(\gamma_1 + \gamma_2 + \gamma_3 + \gamma_4)$	1
$\gamma_s + k(\gamma_5 + \gamma_6 + \gamma_7 + \gamma_8)$	1
$-\gamma_s + (k+1)(\gamma_5 + \gamma_6 + \gamma_7 + \gamma_8)$	1
$\gamma_a + \gamma_b + k\gamma_{D0}$	1
$-\gamma_a - \gamma_b + (k+1)\gamma_{D0}$	1
$\gamma_1 + \gamma_2 + \gamma_3 + \gamma_4 + k\gamma_{D0}$	$y + y^{-1}$
$-\gamma_1 - \gamma_2 - \gamma_3 - \gamma_4 + (k+1)\gamma_{D0}$	$y + y^{-1}$
$(k+1)\gamma_{D0}$	$y^3 + 6y + y^{-1}$

(4.104)

with  $k \geq 0$  and

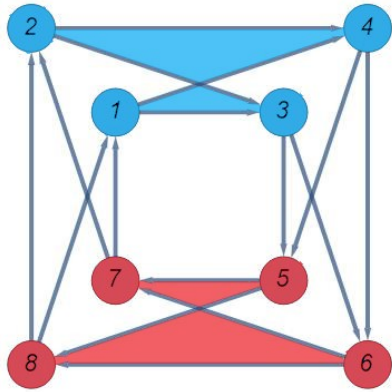
$$\begin{aligned}
r &\in \{1, 2, 3, 4\}, \quad s \in \{5, 6, 7, 8\} \\
(a, b) &\in \{(1, 3), (1, 4), (2, 3), (2, 4), (5, 7), (5, 8), (6, 7), (6, 8)\}
\end{aligned}
\tag{4.105}$$

The spectrum also includes the respective antiparticles obtained by sending  $\gamma \rightarrow -\gamma$ .

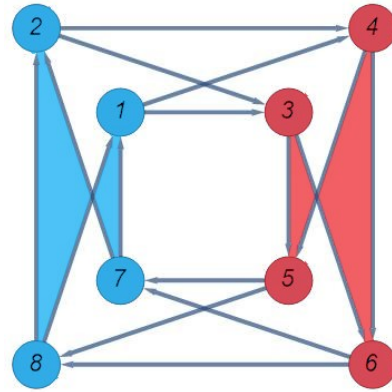
**Remark 7.** *The wall-crossing constraint that we solved is the following identity*

$$\begin{aligned}
&\prod_{k \geq 0}^{\nearrow} \left[ \left( \prod_{\ell=1,2} \Phi(X_{\gamma_\ell + k(\gamma_1 + \gamma_2 + \gamma_3 + \gamma_4)}) \right) \left( \prod_{\ell=5,6} \Phi(X_{\gamma_\ell + k(\gamma_5 + \gamma_6 + \gamma_7 + \gamma_8)}) \right) \right. \\
&\times \left. \left( \prod_{\ell=3,4} \Phi(X_{\gamma_1 + \gamma_2 + \gamma_\ell + k(\gamma_1 + \gamma_2 + \gamma_3 + \gamma_4)}) \right) \left( \prod_{\ell=7,8} \Phi(X_{\gamma_5 + \gamma_6 + \gamma_\ell + k(\gamma_5 + \gamma_6 + \gamma_7 + \gamma_8)}) \right) \right] \\
&\prod_{k \geq 0} \left[ \left( \prod_{s=\pm 1} \Phi((-y)^s X_{\gamma_1 + \gamma_2 + \gamma_3 + \gamma_4 + k\gamma_{D0}})^{-1} \Phi((-y)^s X_{-\gamma_1 - \gamma_2 - \gamma_3 - \gamma_4 + (k+1)\gamma_{D0}})^{-1} \right) \right. \\
&\times \left. \left( \prod_{(a,b)} \Phi(X_{\gamma_a + \gamma_b + k\gamma_{D0}}) \Phi(X_{-\gamma_a - \gamma_b + (k+1)\gamma_{D0}}) \right) \right] \\
&\times \prod_{k \geq 0}^{\searrow} \left[ \left( \prod_{\ell=1,2} \Phi(X_{\gamma_3 + \gamma_4 + \gamma_\ell + k(\gamma_1 + \gamma_2 + \gamma_3 + \gamma_4)}) \right) \left( \prod_{\ell=5,6} \Phi(X_{\gamma_7 + \gamma_8 + \gamma_\ell + k(\gamma_5 + \gamma_6 + \gamma_7 + \gamma_8)}) \right) \right. \\
&\times \left. \left( \prod_{\ell=3,4} \Phi(X_{\gamma_\ell + k(\gamma_1 + \gamma_2 + \gamma_3 + \gamma_4)}) \right) \left( \prod_{\ell=7,8} \Phi(X_{\gamma_\ell + k(\gamma_5 + \gamma_6 + \gamma_7 + \gamma_8)}) \right) \right] \\
&= (\{\gamma_1, \gamma_2, \gamma_3, \gamma_4, \gamma_5, \gamma_6, \gamma_7, \gamma_8\} \rightarrow \{\gamma_3, \gamma_4, \gamma_5, \gamma_6, \gamma_7, \gamma_8, \gamma_1, \gamma_2\})
\end{aligned}
\tag{4.106}$$

where labels  $(a, b)$  run over the same combinations as in (4.105). As we did previously, we factored out the contribution of pure-flavor states (pure  $D0$  branes), which do not participate in wall-crossing. We have tested this as an identity in the numerical ( $y \rightarrow -1$ ) setting, by acting on  $X_{\gamma_i}$  and expanding as formal series in  $X_\gamma$  with  $|\gamma| \leq 10$ .



(a) Four-dimensional subquivers for the flow  $T_1$  of  $dP_5$ .



(b) Four-dimensional subquivers for the flow  $T_2$  of  $dP_5$ .

Figure 18

## References

- [1] D. Gaiotto, G. W. Moore, and A. Neitzke, *Four-dimensional wall-crossing via three-dimensional field theory*, *Commun.Math.Phys.* **299** (2010) 163–224, [[arXiv:0807.4723](#)].
- [2] D. Gaiotto, G. W. Moore, and A. Neitzke, *Wall-crossing, Hitchin systems, and the WKB approximation*, *Adv. Math.* **234** (2013) 239–403, [[arXiv:0907.3987](#)].
- [3] D. Gaiotto, G. W. Moore, and A. Neitzke, *Spectral networks*, *Annales Henri Poincare* **14** (2013) 1643–1731, [[arXiv:1204.4824](#)].
- [4] M. Alim, S. Cecotti, C. Cordova, S. Espahbodi, A. Rastogi, and C. Vafa, *BPS Quivers and Spectra of Complete  $N=2$  Quantum Field Theories*, *Commun. Math. Phys.* **323** (2013) 1185–1227, [[arXiv:1109.4941](#)].
- [5] M. Alim, S. Cecotti, C. Cordova, S. Espahbodi, A. Rastogi, and C. Vafa,  *$\mathcal{N} = 2$  quantum field theories and their BPS quivers*, *Adv. Theor. Math. Phys.* **18** (2014), no. 1 27–127, [[arXiv:1112.3984](#)].
- [6] J. Manschot, B. Pioline, and A. Sen, *Wall Crossing from Boltzmann Black Hole Halos*, *JHEP* **07** (2011) 059, [[arXiv:1011.1258](#)].
- [7] J. Manschot, B. Pioline, and A. Sen, *A Fixed point formula for the index of multi-centered  $N=2$  black holes*, *JHEP* **05** (2011) 057, [[arXiv:1103.1887](#)].
- [8] J. Manschot, B. Pioline, and A. Sen, *From Black Holes to Quivers*, *JHEP* **11** (2012) 023, [[arXiv:1207.2230](#)].
- [9] J. Manschot, B. Pioline, and A. Sen, *On the Coulomb and Higgs branch formulae for multi-centered black holes and quiver invariants*, *JHEP* **05** (2013) 166, [[arXiv:1302.5498](#)].
- [10] J. Manschot, B. Pioline, and A. Sen, *The Coulomb Branch Formula for Quiver Moduli Spaces*, [[arXiv:1404.7154](#)].
- [11] M. Kontsevich and Y. Soibelman, *Stability structures, motivic Donaldson-Thomas invariants and cluster transformations*, [[arXiv:0811.2435](#)].

- [12] D. Joyce and Y. Song, *A Theory of generalized Donaldson-Thomas invariants*, [arXiv:0810.5645](#).
- [13] R. Eager, S. A. Selmani, and J. Walcher, *Exponential Networks and Representations of Quivers*, *JHEP* **08** (2017) 063, [[arXiv:1611.06177](#)].
- [14] S. Banerjee, P. Longhi, and M. Romo, *Exploring 5d BPS Spectra with Exponential Networks*, *Annales Henri Poincaré* **20** (2019), no. 12 4055–4162, [[arXiv:1811.02875](#)].
- [15] S. Banerjee, P. Longhi, and M. Romo, *Exponential BPS graphs and D brane counting on toric Calabi-Yau threefolds: Part I*, [arXiv:1910.05296](#).
- [16] S. Banerjee, P. Longhi, and M. Romo, *Exponential BPS graphs and D-brane counting on toric Calabi-Yau threefolds: Part II*, [arXiv:2012.09769](#).
- [17] C. Closset and M. Del Zotto, *On 5d SCFTs and their BPS quivers. Part I: B-branes and brane tilings*, [arXiv:1912.13502](#).
- [18] P. Bousseau, *Scattering diagrams, stability conditions, and coherent sheaves on  $\mathbb{P}^2$* , [arXiv:1909.02985](#).
- [19] S. Alexandrov and B. Pioline, *Attractor flow trees, BPS indices and quivers*, *Adv. Theor. Math. Phys.* **23** (2019), no. 3 627–699, [[arXiv:1804.06928](#)].
- [20] H. Argüez and P. Bousseau, *The flow tree formula for Donaldson-Thomas invariants of quivers with potentials*, [arXiv:2102.11200](#).
- [21] G. Beaujard, J. Manschot, and B. Pioline, *Vafa-Witten invariants from exceptional collections*, [arXiv:2004.14466](#).
- [22] S. Mozgovoy and B. Pioline, *Attractor invariants, brane tilings and crystals*, [arXiv:2012.14358](#).
- [23] S. Mozgovoy, *Operadic approach to wall-crossing*, [arXiv:2101.07636](#).
- [24] P. Descombes, *Motivic DT invariants from localization*, [arXiv:2106.02518](#).
- [25] P. Longhi, *Wall-Crossing Invariants from Spectral Networks*, [arXiv:1611.00150](#).
- [26] M. Gabella, P. Longhi, C. Y. Park, and M. Yamazaki, *BPS Graphs: From Spectral Networks to BPS Quivers*, [arXiv:1704.04204](#).
- [27] C. Closset and H. Magureanu, *The U-plane of rank-one 4d  $\mathcal{N} = 2$  KK theories*, [arXiv:2107.03509](#).
- [28] M. R. Douglas and G. W. Moore, *D-branes, quivers, and ALE instantons*, [hep-th/9603167](#).
- [29] M. R. Douglas, B. Fiol, and C. Romelsberger, *Stability and BPS branes*, *JHEP* **09** (2005) 006, [[hep-th/0002037](#)].
- [30] M. R. Douglas, B. Fiol, and C. Romelsberger, *The Spectrum of BPS branes on a noncompact Calabi-Yau*, *JHEP* **09** (2005) 057, [[hep-th/0003263](#)].
- [31] F. Denef, *Quantum quivers and Hall / hole halos*, *JHEP* **10** (2002) 023, [[hep-th/0206072](#)].
- [32] W.-y. Chuang, D.-E. Diaconescu, J. Manschot, G. W. Moore, and Y. Soibelman, *Geometric engineering of (framed) BPS states*, *Adv. Theor. Math. Phys.* **18** (2014), no. 5 1063–1231, [[arXiv:1301.3065](#)].
- [33] D. Berenstein and M. R. Douglas, *Seiberg duality for quiver gauge theories*, [hep-th/0207027](#).



- [34] G. Bonelli, F. Del Monte, and A. Tanzini, *BPS quivers of five-dimensional SCFTs, Topological Strings and  $q$ -Painlevé equations*, *Ann. Henri Poincaré* (3, 2021) [[arXiv:2007.11596](#)].
- [35] A. B. Goncharov and R. Kenyon, *Dimers and cluster integrable systems*, [arXiv:1107.5588](#).
- [36] V. V. Fock and A. Marshakov, *Loop groups, Clusters, Dimers and Integrable systems*, [arXiv:1401.1606](#).
- [37] M. Bershtein, P. Gavrylenko, and A. Marshakov, *Cluster integrable systems,  $q$ -Painlevé equations and their quantization*, *JHEP* **02** (2018) 077, [[arXiv:1711.02063](#)].
- [38] Y. Mizuno,  *$q$ -painlevé equations on cluster  $\mathcal{X}$ -varieties via toric geometry*, *arXiv preprint arXiv:2008.11219* (2020).
- [39] M. A. Bershtein and A. I. Shchepochkin,  *$q$ -deformed Painlevé  $\tau$  function and  $q$ -deformed conformal blocks*, *J. Phys. A* **50** (2017), no. 8 085202, [[arXiv:1608.02566](#)].
- [40] G. Bonelli, A. Grassi, and A. Tanzini, *Quantum curves and  $q$ -deformed Painlevé equations*, *Lett. Math. Phys.* **109** (2019), no. 9 1961–2001, [[arXiv:1710.11603](#)].
- [41] P. Longhi, *Instanton Particles and Monopole Strings in 5D  $SU(2)$  Supersymmetric Yang-Mills Theory*, *Phys. Rev. Lett.* **126** (2021), no. 21 211601, [[arXiv:2101.01681](#)].
- [42] H. Sakai, *Rational Surfaces Associated with Affine Root Systems and Geometry of the Painlevé Equations*, *Communications in Mathematical Physics* **220** (Jan., 2001) 165–229.
- [43] S. Cecotti and M. Del Zotto,  *$Y$  systems,  $Q$  systems, and 4D  $\mathcal{N} = 2$  supersymmetric QFT*, *J. Phys. A* **47** (2014), no. 47 474001, [[arXiv:1403.7613](#)].
- [44] M. Cirafici and M. Del Zotto, *Discrete Integrable Systems, Supersymmetric Quantum Mechanics, and Framed BPS States - I*, [arXiv:1703.04786](#).
- [45] M. Cirafici, *A note on discrete dynamical systems in theories of class  $S$* , *JHEP* **05** (2021) 224, [[arXiv:2011.12887](#)].
- [46] J. Gu and M. Mariño, *Peacock patterns and new integer invariants in topological string theory*, [arXiv:2104.07437](#).
- [47] A. King, *Moduli of representations of finite dimensional algebras*, *Quarterly Journal of Mathematics* **45** (1994) 515–530.
- [48] T. Bridgeland, *Stability conditions on triangulated categories*, *arXiv Mathematics e-prints* (Dec., 2002) math/0212237, [[math/0212237](#)].
- [49] T. Bridgeland, *Scattering diagrams, Hall algebras and stability conditions*, *arXiv e-prints* (Mar., 2016) arXiv:1603.00416, [[arXiv:1603.00416](#)].
- [50] M. R. Douglas, *Dirichlet branes, homological mirror symmetry, and stability*, [math/0207021](#).
- [51] M. R. Douglas,  *$D$ -Branes on Calabi-Yau Manifolds*, *arXiv Mathematics e-prints* (Sept., 2000) math/0009209, [[math/0009209](#)].
- [52] M. R. Douglas,  *$D$ -branes, categories and  $N=1$  supersymmetry*, *J. Math. Phys.* **42** (2001) 2818–2843, [[hep-th/0011017](#)].
- [53] P. Yi, *Witten index and threshold bound states of  $D$ -branes*, *Nucl. Phys. B* **505** (1997) 307–318, [[hep-th/9704098](#)].
- [54] Z. Duan, D. Ghim, and P. Yi, *5D BPS Quivers and KK Towers*, [arXiv:2011.04661](#).

- [55] D. Gaiotto, G. W. Moore, and A. Neitzke, *Framed BPS States*, *Adv.Theor.Math.Phys.* **17** (2013) 241–397, [[arXiv:1006.0146](#)].
- [56] N. Seiberg and E. Witten, *Electric - magnetic duality, monopole condensation, and confinement in  $N=2$  supersymmetric Yang-Mills theory*, *Nucl. Phys.* **B426** (1994) 19–52, [[hep-th/9407087](#)]. [Erratum: *Nucl. Phys.*B430,485(1994)].
- [57] P. Longhi, *The structure of BPS spectra*. PhD thesis, Rutgers U., Piscataway, 2015.
- [58] N. Seiberg, *Five-dimensional SUSY field theories, nontrivial fixed points and string dynamics*, *Phys. Lett. B* **388** (1996) 753–760, [[hep-th/9608111](#)].
- [59] K. A. Intriligator, D. R. Morrison, and N. Seiberg, *Five-dimensional supersymmetric gauge theories and degenerations of Calabi-Yau spaces*, *Nucl. Phys. B* **497** (1997) 56–100, [[hep-th/9702198](#)].
- [60] C. Closset, M. Del Zotto, and V. Saxena, *Five-dimensional SCFTs and gauge theory phases: an M-theory/type IIA perspective*, *SciPost Phys.* **6** (2019), no. 5 052, [[arXiv:1812.10451](#)].
- [61] A. Iqbal, A. Neitzke, and C. Vafa, *A Mysterious duality*, *Adv. Theor. Math. Phys.* **5** (2002) 769–808, [[hep-th/0111068](#)].
- [62] A. Hanany and A. Iqbal, *Quiver theories from D6 branes via mirror symmetry*, *JHEP* **04** (2002) 009, [[hep-th/0108137](#)].
- [63] N. Joshi, *Discrete Painlevé Equations*. CBMS Regional Conference Series in Mathematics. Conference Board of the Mathematical Sciences, 2019.
- [64] M. Gross, P. Hacking, and S. Keel, *Moduli of surfaces with an anti-canonical cycle*, *Compositio Mathematica* **151** (2015), no. 2 265–291.
- [65] S. Cecotti and C. Vafa, *Classification of complete  $N=2$  supersymmetric theories in 4 dimensions*, *Surveys in differential geometry* **18** (2013) [[arXiv:1103.5832](#)].
- [66] S. Franco, Y.-H. He, C. Sun, and Y. Xiao, *A Comprehensive Survey of Brane Tilings*, *Int. J. Mod. Phys. A* **32** (2017), no. 23n24 1750142, [[arXiv:1702.03958](#)].
- [67] A. Klemm, W. Lerche, P. Mayr, C. Vafa, and N. P. Warner, *Selfdual strings and  $N=2$  supersymmetric field theory*, *Nucl. Phys.* **B477** (1996) 746–766, [[hep-th/9604034](#)].
- [68] K. Kajiwara, M. Noumi, and Y. Yamada, *Geometric Aspects of Painlevé Equations*, *arXiv e-prints* (Sept., 2015) arXiv:1509.08186, [[arXiv:1509.08186](#)].
- [69] K.-M. Lee and P. Yi, *Monopoles and instantons on partially compactified D-branes*, *Phys. Rev. D* **56** (1997) 3711–3717, [[hep-th/9702107](#)].
- [70] M. Wijnholt, *Large volume perspective on branes at singularities*, *Adv. Theor. Math. Phys.* **7** (2003), no. 6 1117–1153, [[hep-th/0212021](#)].
- [71] A. Hanany and R.-K. Seong, *Brane Tilings and Reflexive Polygons*, *Fortsch. Phys.* **60** (2012) 695–803, [[arXiv:1201.2614](#)].